

## Evolutionary Covariation in Geometric Morphometric Data: Analyzing Integration, Modularity, and Allometry in a Phylogenetic Context

CHRISTIAN PETER KLINGENBERG<sup>1</sup> AND JESÚS MARUGÁN-LOBÓN<sup>2</sup>

<sup>1</sup>Faculty of Life Sciences, University of Manchester, Michael Smith Building, Oxford Road, Manchester M13 9PT, UK; and <sup>2</sup>Unidad de Paleontología, Departamento de Biología, C/Darwin 2, Universidad Autónoma de Madrid, Cantoblanco, 28049 Madrid, Spain;

\*Correspondence to be sent to Christian Peter Klingenberg; E-mail: cpk@manchester.ac.uk.

Received 13 September 2012; reviews returned 11 December 2012; accepted 6 April 2013

Associate Editor: Norm MacLeod

**Abstract.**—Quantifying integration and modularity of evolutionary changes in morphometric traits is crucial for understanding how organismal shapes evolve. For this purpose, comparative studies are necessary, which need to take into account the phylogenetic structure of interspecific data. This study applies several of the standard tools of geometric morphometrics, which mostly have been used in intraspecific studies, in the new context of analyzing integration and modularity based on comparative data. Morphometric methods such as principal component analysis, multivariate regression, partial least squares, and modularity tests can be applied to phylogenetically independent contrasts of shape data. We illustrate this approach in an analysis of cranial evolution in 160 species from all orders of birds. Mapping the shape information onto the phylogeny indicates that there is a significant phylogenetic signal in skull shape. Multivariate regression of independent contrasts of shape on independent contrasts of size reveals clear evolutionary allometry. Regardless of whether or not a correction for allometry is used, evolutionary integration between the face and braincase is strong, and tests reject the hypothesis that the face and braincase are separate evolutionary modules. These analyses can easily be applied to other taxa and can be combined with other morphometric tools to address a wide range of questions about evolutionary patterns and processes. [Aves; comparative methods; independent contrasts; morphological integration; partial least squares; Procrustes superimposition; shape; skull.]

The parts of organisms do not evolve in isolation from each other, but are integrated with one another to various degrees. This integration is not uniform throughout entire organisms, but is usually organized in a modular manner, with complexes of tightly integrated parts, or modules, that are relatively independent from each other (Olson and Miller 1958; Cheverud 1996; Chernoff and Magwene 1999; Schlosser and Wagner 2004; Klingenberg 2008). Much of the discussion of integration and modularity has been concerned with the structure of intraspecific variation, both genetic and phenotypic, which is crucial for evolution by selection or drift (Felsenstein 1988; Wagner and Altenberg 1996). Morphological integration, however, is also manifest at a macroevolutionary level. At this level, it reflects the way in which evolutionary changes in different parts of organisms are associated (Klingenberg 2008, 2013). Integration at the macroevolutionary level can manifest itself as evolutionary trends or constraints, so that evolutionary divergence occurs primarily in some directions in phenotypic space (Gould 1989; Arthur 2001; Hunt 2007; Sidlauskas 2008). Likewise, modularity at this level refers to complexes of traits that evolve in relative independence of each other (Monteiro et al. 2005; Klingenberg 2008). By relating the patterns of integration and modularity at the macroevolutionary level to the patterns of variation within taxa, it is possible to make inferences on the mechanisms that generate evolutionary change (Monteiro et al. 2005; Breuker et al. 2006; Bastir 2008; Klingenberg 2008, 2010, 2013).

To study integration at the evolutionary level, it is necessary to adopt a comparative approach that

takes into account the phylogenetic structure of the data (Felsenstein 1985; Harvey and Pagel 1991; Garland et al. 2005; Monteiro 2013) and to combine it with the morphometric methods for investigating integration and modularity, which so far have mostly been used for characterizing morphological integration and modularity within species (e.g., Monteiro and Abe 1997; Klingenberg and Zaklan 2000; Klingenberg et al. 2001; 2003; Bookstein et al. 2003; Bastir and Rosas 2006; Goswami 2006a; Young and Badyaev 2006; Mitteroecker and Bookstein 2008; Zelditch et al. 2008; Hallgrímsson et al. 2009; Klingenberg 2009; Kulemeyer et al. 2009; Laffont et al. 2009; Goswami and Polly 2010; Ivanović and Kalezić 2010; Bastir et al. 2011; Jammniczky and Hallgrímsson 2011; Jojić et al. 2011, 2012; Martínez-Abadías et al. 2011, 2012; Parsons et al. 2011; Webster and Zelditch 2011; Kimmel et al. 2012; Sanger et al. 2012; Neaux et al. 2013a; 2013b; Wellens et al. 2013). Some studies have used special techniques, such as matrix correlation between matrices of shape distances among taxa for different parts (Monteiro et al. 2005; Monteiro and Nogueira 2010; Muñoz-Muñoz et al. 2011), or partial least squares (PLS) analysis across species without adjustment for phylogenetic structure in the data (Monteiro et al. 2005; Marugán-Lobón and Buscalioni 2006; Márquez and Knowles 2007; Hautier et al. 2012; Chamero et al. 2013). A few studies have used explicit phylogenetic approaches such as regression of independent contrasts or phylogenetic generalized least squares (PGLS) regression for studying evolutionary allometry (Meloro et al. 2008; Gonzalez et al. 2011; Perez et al. 2011; García and Sarmiento

2012; Klingenberg et al. 2012). Although regression analysis has been the main focus of attention in the literature on comparative methods (Felsenstein 1985; Harvey and Pagel 1991; Martins and Hansen 1997; Rohlf 2001,2006; Blomberg et al. 2012), there is no inherent limitation in phylogenetic comparative approaches that restricts them to regression. To the contrary, all the usual tools of geometric morphometrics can be used in a phylogenetic comparative context (Monteiro 2013). Here, we present an approach that uses a range of geometric morphometric methods to study how evolutionary changes in a complex morphological structure are integrated in a major evolving clade.

We use the skull of birds as a model system. Birds have a remarkable variety of skull morphologies (Zusi 1993), but only a few studies have used the methods of geometric morphometrics to analyze this variation within particular groups (Acosta Hospitaleche and Tambussi 2006; van der Meij and Bout 2008; Brusaferrero and Insom 2009; Kulemeyer et al. 2009; Degrange and Picasso 2010) or across the entire range of birds (Marugán-Lobón and Buscalioni 2004, 2006, 2009; Marugán-Lobón 2010). A recent morphometric analysis indicates that pedomorphosis was an important factor in the evolution of the skull shape of birds (Bhullar et al. 2012). Cranial shape has also been shown to be associated with bite force and other aspects of mechanical performance in birds (Herrel et al. 2005, 2010; van der Meij and Bout 2008; Rayfield 2011) and other animals (Pierce et al. 2008; Nogueira et al. 2009; Fortuny et al. 2011; O'Higgins et al. 2011; Brusatte et al. 2012; Kleinteich et al. 2012). Although pedomorphosis is expected to lead to integrated evolution of the skull as a whole, adaptive evolution for different functions may produce differential changes in different parts of the skull such as the beak, orbit, and braincase. We make use of progress in avian phylogenetics (Hackett et al. 2008; Mayr 2011) and a combination of geometric morphometric methods to address the question whether evolution of the skull in birds is integrated or whether cranial regions evolve as distinct modules.

Here, we apply several methods for investigating morphological integration and modularity in the new context of large-scale phylogeny. This study is the first to demonstrate that a wide range of morphometric methods can be combined with phylogenetic comparative methods to apply them in the context of evolutionary integration and modularity, which is concerned with the covariation among the evolutionary changes in the parts of morphological structures. We investigate different aspects of evolutionary integration and modularity by applying principal component analysis (PCA) (e.g., Jolliffe 2002), multivariate regression for characterizing allometry (Monteiro 1999), PLS analysis (Rohlf and Corti 2000), and tests of modularity (Klingenberg 2009) to phylogenetically independent contrasts of shape data (Felsenstein 1985; Rohlf 2001). The coordinated use of this array of morphometric tools makes it possible to gain a comprehensive and multifaceted view of integration

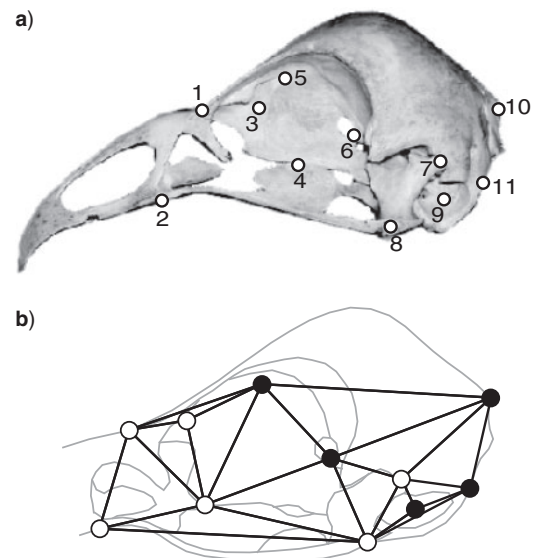


FIGURE 1. Landmarks used in this study and their subdivision into subsets for the face and braincase. a) The landmarks used in this study. They are the same as in an earlier study, which also included an additional landmark at the tip of the beak (for definitions of landmarks, see Marugán-Lobón and Buscalioni (2006), but note the difference in the numbering scheme). b) Partition of the landmarks into subsets corresponding to the face (white circles) and braincase (black circles). The black lines represent the adjacency graph used for defining spatially contiguous partitions of landmarks in the test of modularity (Klingenberg 2009).

and modularity, which we apply to the evolution of avian skulls.

## METHODS

### *Morphometric Data*

A set of 12 landmarks were digitized in lateral views of the skulls of 160 species of birds (for anatomical descriptions of landmarks, see Marugán-Lobón and Buscalioni 2006). Because the landmark at the tip of the beak reflects a large amount of variation in the beak (mostly in the premaxilla; Marugán-Lobón and Buscalioni 2004), which would obscure other patterns of cranial variation that are of primary interest for this study, we omit this landmark and focus on the remaining 11 landmarks covering the midface and neurocranium (Fig. 1).

Shape information was extracted from the landmark coordinates with a generalized full Procrustes fit (Dryden and Mardia 1998). For the few species with multiple specimens in the data set, the average shape was used in the analyses. Estimates of shape variation among species contain a component of intraspecific variation and measurement error, although we are confident that this component is small relative to the large scale of differences among taxa. For studies with larger samples per species, there are methods for quantifying this component explicitly and correcting for its effect in comparative analyses (Ives et al. 2007; Felsenstein 2008).

All morphometric analyses were conducted with the MorphoJ software (Klingenberg 2011).

### Phylogeny and Comparative Approach

The comparative analyses in this study are based on the phylogenetic tree of Hackett et al. (2008), which is a molecular phylogeny of birds that combines extensive taxon coverage and a high number of loci sequenced and is widely used as backbone phylogeny in comparative studies (for discussion, see Mayr 2011; Pacheco et al. 2011; Jetz et al. 2012; McCormack et al. 2013). This tree was augmented with additional information from phylogenetic studies of specific subgroups (Barker and Lanyon 2000; Sheldon et al. 2000; Wink and Heidrich 2000; Lerner and Mindell 2005; Pons et al. 2005; Benz et al. 2006; Jönsson and Fjeldså 2006; Moyle 2006; Baker et al. 2007; Fain et al. 2007; Treplin et al. 2008; Wright et al. 2008; Eo et al. 2009; Phillips et al. 2010). The resulting composite phylogeny (Fig. 2) was used for mapping shape data by squared-change parsimony (Maddison 1991; McArdle and Rodrigo 1994; Klingenberg and Ekau 1996; Sidlauskas 2008; Klingenberg and Gidaszewski 2010) and to compute independent contrasts (Felsenstein 1985).

Because of the composite nature of this tree, branch lengths were not available for all branches. Therefore, all branch lengths were set to the same length (i.e., assuming an evolutionary model with the same expected amount of morphological change on every branch). This means we used unweighted squared-change parsimony (Maddison 1991) and its equivalent for independent contrasts. To evaluate whether the results were sensitive to this arbitrary choice of equal branch lengths, we also ran analyses using a different set of branch lengths that were chosen so that the resulting tree was ultrametric (using the Mesquite software; Maddison and Maddison 2011). The results from analyses based on those branch lengths were very similar to the results using equal branch lengths, so that it appears that the main conclusions of this study are robust with regard to the choice of branch lengths.

To investigate whether the morphometric data contain a phylogenetic signal, we used a permutation approach (Klingenberg and Gidaszewski 2010). This test simulates the null hypothesis of no phylogenetic signal in the data by randomly exchanging the shape data among the tips of the phylogenetic tree. We used 10 000 random permutations for the test. A significant test indicates that the data have a phylogenetic structure, which needs to be taken into account by all further comparative analyses.

Phylogenetically independent contrasts for multivariate features like shape can be computed in the same way as for scalar variables, as weighted differences of observed or reconstructed values for sister nodes (Felsenstein 1985; Rohlf 2001). Note that the reconstructions of values for internal nodes are not globally optimized across the entire tree as for squared-change parsimony, but only take into account

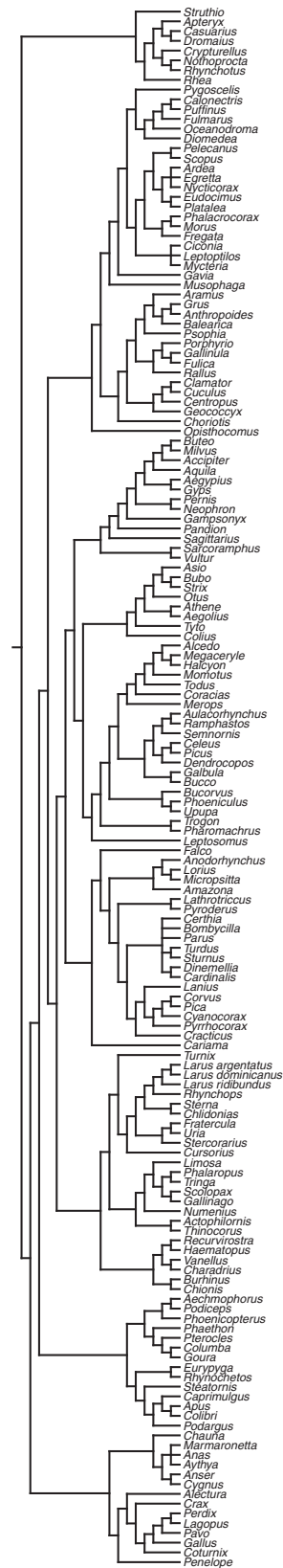


FIGURE 2. Phylogeny used in this study. The tree is mostly based on the phylogeny of Hackett et al. (2008), with additional information from other sources (see text for details).

the descendants of each internal node as the algorithm passes down the tree from the terminal taxa to the root (Felsenstein 1985; Garland et al. 1999; Rohlf 2001). In the context of shape, vectors of Procrustes coordinates are used as the data, but the weighting coefficients for each node are the same for all variables at each node and are identical to those used in univariate computations (computations can be done conveniently in matrix form; Rohlf 2001). Polytomies can be resolved by inserting zero-length branches in the tree (Felsenstein 1985; Purvis and Garland 1993; Rohlf 2001).

#### *Patterns of Evolutionary Diversification in Shape Space*

To reconstruct and visualize the phylogenetic history of shape change, we project the phylogeny into the shape tangent space and draw it on plots of multivariate ordinations of species means. This approach provides intuitive graphical displays that show, as far as it is possible to infer from the shape information of terminal taxa, how specific clades diversified and spread through the space of morphometric variables (e.g., Klingenberg and Ekau 1996; Linde et al. 2004; Sidlauskas 2008; Figueirido et al. 2010, 2013; Klingenberg and Gidaszewski 2010; De Esteban-Trivigno 2011a, 2011b; Dornburg et al. 2011; Fortuny et al. 2011; Monteiro and Nogueira 2011; Brusatte et al. 2012; Klingenberg et al. 2012; Meloro and Jones 2012; Chamero et al. 2013).

For these plots, the shapes corresponding to the internal nodes of the phylogeny are reconstructed by squared-change parsimony (Maddison 1991; McArdle and Rodrigo 1994). We display the projected tree in scatter plots of principal component (PC) scores from a PCA computed from the covariance matrix among the average shapes of the terminal taxa. Because specific lineages and clades are the focus of these displays, not the overall evolutionary process, these analyses are using species means and not independent contrasts as the units of analysis.

These analyses were conducted for both the original shape space and the space of the data after size correction to remove the effects of evolutionary allometry. Any large differences between the two analyses would indicate that evolutionary allometry is an important factor for cranial evolution in birds.

#### *Evolutionary Allometry and Size Correction*

Allometry, the variation in shape that is associated with variation in size (Gould 1966; Mosimann 1970), is a factor that can contribute substantially to integration of morphological traits. In geometric morphometrics, allometry is widely characterized by multivariate regression of shape on size (usually centroid size or log-transformed centroid size); such regressions often fit the data well and the allometric shape changes tend to affect the entire structures under study (e.g., Loy et al. 1996, 1998; Monteiro and Abe 1997; Monteiro 1999; Klingenberg et al. 2001; Mitteroecker et al. 2004,

Rosas and Bastir 2004; Drake and Klingenberg 2008; Gidaszewski et al. 2009; Kulemeyer et al. 2009; Adams and Nistri 2010; Figueirido et al. 2010; Gonzalez et al. 2010, 2013; Bastir et al. 2011; Rodríguez-Mendoza et al. 2011; Sidlauskas et al. 2011; Weisensee and Jantz 2011; Bhullar et al. 2012; Klingenberg et al. 2012; Ponssa and Candiotti 2012; Neaux et al. 2013b; Wellens et al. 2013). Due to the linear or near-linear relationship between shape and size, the allometric effects of size variation are concentrated in a single dimension of the shape tangent space and, because allometric variation can amount to a sizeable proportion of total shape variation, allometry can contribute substantially to overall integration of shape (Rosas and Bastir 2004; Klingenberg 2008, 2009, 2013). Equivalently, in the framework of factor analysis (e.g., Bookstein et al. 1985; Mitteroecker and Bookstein 2007), the allometric effects of size variation are considered as a common factor. The logic that integration is the degree to which variation is concentrated in one or a few dimensions also is the foundation for indices of integration based on the variance of eigenvalues of a correlation or covariance matrix (e.g., Wagner 1984; Willmore et al. 2006; Young 2006; Pavlicev et al. 2009; Haber 2011; Klingenberg 2013).

In the context of diversification among taxa, the focus is on evolutionary allometry, the evolutionary change of shape that is associated with evolutionary change of size (Cock 1966; Klingenberg 1996). To characterize evolutionary allometry, we use a multivariate regression of independent contrasts of shape on independent contrasts of size. This is an adaptation of the method using multivariate regression (e.g., Monteiro 1999), modified for the context of evolutionary allometry by using independent contrasts as the units of the analysis (Figueirido et al. 2010; Perez et al. 2011; Klingenberg et al. 2012). This approach, based on independent contrasts, is equivalent to the analysis using regression in the framework of phylogenetic generalized linear models (Meloro et al. 2008; Gonzalez et al. 2011; Álvarez and Perez 2013; Blomberg et al. 2012). A simplified method, where shape information was reduced to PC1 scores, has also been used for characterizing evolutionary allometry with independent contrasts (García and Sarmiento 2012).

To estimate evolutionary allometry, we use multivariate regression of the independent contrasts of Procrustes coordinates, as the shape variables, on independent contrasts of log-transformed centroid size, as the size measure. Because the ordering of sister nodes in the tree is arbitrary, it is necessary to use a regression through the origin for the analysis of independent contrasts (Garland et al. 1992; Rohlf 2001). The residuals resulting from this regression can be used in a variety of analyses for studying aspects of morphometric integration and modularity (e.g., Klingenberg 2009).

In some analyses, however, the original shape data for the taxa, rather than the contrasts, are the primary focus of interest. To eliminate the effect of evolutionary allometry, the size correction based on the regression of independent contrasts can also be applied to species averages or similar statistics. For this purpose, the vector

of regression coefficients computed from independent contrasts is used to decompose the deviations of species' mean shapes from the grand mean into predicted and residual components (this is similar to the method for phylogenetic size correction described by Revell [2009]).

#### *Patterns of Variation in Evolutionary Shape Changes*

Morphological integration across species arises from associations among aspects of shape in the evolutionary changes along the branches of the phylogeny. This integration can be studied by examining patterns of variation in the covariance matrix of independent contrasts for cranial shape. PCA is a useful technique in this context, as the first few eigenvectors (vectors of PC coefficients) identify the dominant features of shape variation and the corresponding eigenvalues indicate the amount of variation associated with each PC (e.g., Pearson 1901; Jolliffe 2002).

The covariance matrix of independent contrasts is computed without centering, so that it is the same regardless of the arbitrary ordering of sister nodes from which independent contrasts are computed (this is equivalent to the arbitrary sign of univariate contrasts). As another consequence of this, scatter plots of PC scores for independent contrasts are not very informative (the position of each data point is only determined up to a rotation by 180° about the origin, and there are therefore many equivalent arrangements of data points that superficially may appear very different). The eigenvectors and eigenvalues, however, can be interpreted in the same way as for PCA in other contexts.

This analysis is equivalent to the phylogenetic PCA proposed by Revell 2009, but uses a different algorithm to estimate the covariance matrix from which PCs are extracted (independent contrasts instead of PGLS—but recall that both methods are equivalent; Rohlf 2001; Blomberg et al. 2012). In the context of geometric morphometrics, by contrast to Revell's general algorithm, it is important to use the covariance and not the correlation matrix for the analysis, because the scaling of variables needs to be preserved across all coordinates of all landmarks (Klingenberg and Zaklan 2000).

#### *Evolutionary Integration between Face and Braincase: PLS*

To characterize the patterns of integration between the braincase and face, we use PLS analysis (Bookstein 1991; Rohlf and Corti 2000). PLS was first used in psychometrics under the name "inter-battery factor analysis" (Tucker 1958) and first has been used in geometric morphometrics mostly to relate results from different analyses and in ecomorphology (Tabachnick and Bookstein 1990; Adams and Rohlf 2000; Corti and Rohlf 2001). In the last decade, PLS has been used increasingly for characterizing patterns of

morphological integration (e.g., Klingenberg and Zaklan 2000; Klingenberg et al. 2001, 2003; Bookstein et al. 2003; Bastir and Rosas 2005, 2006; Monteiro et al. 2005; Marugán-Lobón and Buscalioni 2006; Mitteroecker and Bookstein 2008; Kulemeyer et al. 2009; Laffont et al. 2009; Gkantidis and Halazonetis 2011; Gómez-Robles et al. 2011; Jamniczky and Hallgrímsson 2011; Martínez-Abadías et al. 2011; Parsons et al. 2011; Hautier et al. 2012; Makedonska et al. 2012; Renaud et al. 2012; Singh et al. 2012; Chamero et al. 2013; Neaux et al. 2013a; 2013b). PLS analysis uses a singular value decomposition of the matrix of covariances between two sets of variables to extract pairs of PLS axes, one for each set, that have maximum covariance with each other and provide a summary of the total covariation between sets in a minimum number of dimensions (Rohlf and Corti 2000). PLS analysis differs from canonical correlation analysis, which is better known outside of geometric morphometrics and finds pairs of axes that maximize correlation rather than covariance (e.g., Mardia et al. 1979); in geometric morphometrics, this would be problematic because of the rescaling that is involved in the computations (for a more detailed comparison, see Rohlf and Corti 2000).

To analyze the covariation of evolutionary changes between the face and braincase (Fig. 1), the PLS analysis uses the independent contrasts of the shape variables. Because independent contrasts represent evolutionary change, the covariation between independent contrasts of the shape coordinates for face and braincase indicates evolutionary integration of shape between them. PLS axes computed from independent contrasts therefore identify shape features with maximal evolutionary covariation.

To analyze the patterns of integration between the braincase and face as parts of the skull as a whole, we conduct a PLS analysis of the shape coordinates from a simultaneous Procrustes fit for the entire landmark configuration (e.g., Klingenberg and Zaklan 2000; Bookstein et al. 2003; Klingenberg et al. 2003; Monteiro et al. 2005; Mitteroecker and Bookstein 2008; Kulemeyer et al. 2009; McCane and Kean 2011; Makedonska et al. 2012). This approach considers covariation that originates from coordinated variation in the shapes of the parts as well as covariation that stems from variation in the relative sizes and positioning of the parts. An alternative option is to divide the configuration of landmarks into separate sets for the parts, to compute a separate Procrustes superimposition for each of the parts, and to use the resulting blocks of shape coordinates in a PLS analysis between parts (e.g., Bastir and Rosas 2005; 2006; Marugán-Lobón and Buscalioni 2006; Kulemeyer et al. 2009; Laffont et al. 2009; Gkantidis and Halazonetis 2011; Jamniczky and Hallgrímsson 2011; Martínez-Abadías et al. 2011; Parsons et al. 2011; Singh et al. 2012; Neaux et al. 2013a; 2013b). This latter approach considers the integration between the shapes of parts considered separately but excludes all covariation that originates from coordinated variation in the relative sizes, positions, and orientations of the parts.

Both approaches are feasible in an evolutionary context, with independent contrasts as the data. The difference between these two approaches can be substantial (Klingenberg 2009; Kulemeyer et al. 2009; McCane and Kean 2011), and it is therefore important to consider the particular context for each study to determine which approach is more appropriate. Because this study aims to consider all aspects of integration throughout the skull, including effects of coordinated changes in the relative sizes and positioning of the face and braincase, we use the approach with a simultaneous Procrustes fit for the whole landmark configuration.

Each pair of PLS axes for the face and braincase is computed as a pair of separate vectors from the singular value decomposition of the matrix of covariances between blocks (e.g., Rohlf and Corti 2000). However, for producing graphs of the corresponding shape changes and for comparisons with other analyses such as the PCA of the entire configuration or allometric regression, the two vectors of each pair need to be combined. For this purpose, the coefficients of the two PLS axes in each pair must be scaled relative to each other in some meaningful way (Klingenberg and Zaklan 2000; Monteiro et al. 2005; Mitteroecker and Bookstein 2008). We used the algorithm of Mitteroecker and Bookstein (2008, Appendix) for obtaining the scaling factors for the two blocks of variables and each pair of PLS axes.

For the PLS analysis of independent contrasts, the singular value decomposition is computed from an uncentered covariance matrix, so that the results are unaffected by the arbitrary ordering of sister nodes from which the contrasts are obtained (implemented in the MorphoJ software from version 1.04b on; Klingenberg 2011). The interpretation of the results from the PLS analysis is as usual for the shape changes and the amounts of covariation associated with the different PLS axes. For the scatter plots of PLS scores in the different blocks, however, the arbitrary ordering of sister nodes introduces some ambiguity (the position of each data point is only determined up to a rotation by 180° around the origin of the plot). It is therefore helpful to use other ways to present the strength of association for pairs of PLS axes (e.g., percentages of total squared covariances for which pairs of PLS axes account, correlation of PLS scores, or the RV coefficient of overall association).

To quantify the strength of the overall association between the face and the braincase, we use the RV coefficient (Escoufier 1973; Klingenberg 2009). The RV coefficient is a measure of association between two sets of variables that can be viewed as a multivariate generalization of the squared correlation coefficient. It takes values from 0 for complete independence between sets to 1 for total interdependence where variation in each set is perfectly predictable from variation in the other set. The RV coefficient has been used as a measure of integration between parts in a growing number of studies (e.g., Klingenberg 2009; Laffont et al. 2009; Gómez-Robles et al. 2011; Parsons et al. 2011; Gómez-Robles and Polly 2012).

To test the covariation between face and braincase, we use a permutation test (Good 2000; Manly 2007) against the null hypothesis of total independence. This test simulates the null hypothesis by randomly reshuffling observations separately within the blocks of landmark coordinates for the face and braincase (Fig. 1) and uses the RV coefficient as the test statistic. For statistical tests of covariation between parts of a configuration of landmarks, it is important to note that a simultaneous Procrustes fit of all parts causes some covariation itself and therefore needs to be taken into account explicitly (Klingenberg et al. 2003; Klingenberg 2009). In each round of the permutation procedure, when the landmark coordinates of the face and braincase have been reshuffled and randomly combined from different skulls, the newly combined configurations are likely to vary slightly in size, position, and orientation. To remove this component of nonshape variation, each iteration of the permutation procedure needs to include a new Procrustes superimposition (Klingenberg et al. 2003; Klingenberg 2009). A further complication is that the observations are the independent contrasts of Procrustes coordinates. Because independent contrasts are shape changes rather than shapes and have an average very near to zero for every coordinate, they cannot be used directly in the Procrustes superimposition. Therefore, the mean shape needs to be added to the vectors of independent contrasts for the Procrustes fits as part of the permutation procedure (this is analogous to the permutation procedure for other types of shape changes, e.g., fluctuating asymmetry; Klingenberg et al. 2003; Klingenberg 2009). To facilitate fast convergence of the algorithm for the generalized Procrustes superimposition (Goodall 1991; Dryden and Mardia 1998), the mean shape can be used as the target in the initial iteration (the mean shape of permuted shapes is expected to be very close to the original mean shape). These modifications of the permutation test are implemented in the MorphoJ software (Klingenberg 2011) and are used automatically in appropriate situations.

#### *Angular Comparisons of Results from PCA, PLS, and Regression*

Visualizations of shape changes associated with results from statistical analyses such as PCA, PLS, or regression often suggest that vectors are similar or even identical. For instance, if allometry accounts for most of the variation, the allometric regression vector from a regression of shape on size might be expected to coincide with the PC1. To assess such impressions quantitatively, we used angular comparisons between the vectors in question. Angles between vectors are a direct and intuitive measure of the similarity of two vectors in shape tangent space or a similar multidimensional space (e.g., Cheverud 1982b; Klingenberg and Zimmermann 1992; Klingenberg and McIntyre 1998; Klingenberg and Zaklan 2000; Klingenberg et al. 2001, 2003; Strand

Viðarsdóttir et al. 2002; Rosas and Bastir 2004; Gonzalez et al. 2010; Rodríguez-Mendoza et al. 2011; Ponssa and Candiotti 2012). The angle  $\alpha$  between two vectors, written as column vectors  $\mathbf{a}$  and  $\mathbf{b}$ , can be computed as  $\alpha = \arccos(\mathbf{a}^T \mathbf{b} / (\mathbf{a}^T \mathbf{a} \times \mathbf{b}^T \mathbf{b})^{-0.5})$ , where the superscript “ $T$ ” denotes the transpose.

To assess the angles between pairs of vectors statistically, many authors have used Monte Carlo simulation to generate the distribution of angles between pairs of random vectors in the hyperspace of the appropriate dimensionality (e.g., Cheverud 1982b; Klingenberg and Zimmermann 1992; Klingenberg and McIntyre 1998; Drake and Klingenberg 2008). These simulations can be time consuming and produce only approximate  $P$ -values. There is an alternative, however, as Li (2011) has published a closed-form expression for the area of the cap of a hypersphere. The cap of the hypersphere is the portion of the surface that is within a certain angle  $\alpha$  of a fixed vector. The area of the cap divided by the area of the entire hypersphere is the probability that a random vector drawn from a uniform distribution forms an angle with the fixed vector that equals  $\alpha$  or is less (i.e., this ratio is the required  $P$ -value). The formula is based on the regularized incomplete beta function, which is available in many numerical software libraries (for mathematical details, see Li [2011]).

For vectors such as PC and PLS axes, where the direction of the vectors is arbitrary, angles were computed as  $\alpha = \arccos(\text{abs}(\mathbf{a}^T \mathbf{b}))$ , which limits the angles to a range between  $0^\circ$  and  $90^\circ$  (note also that PC and PLS axes are scaled so that  $\mathbf{a}^T \mathbf{a} = 1$  and  $\mathbf{b}^T \mathbf{b} = 1$ ). Accordingly, the computations of angles between random vectors only consider a hemi-hypersphere. Angular comparisons and the statistical comparisons to angles between random vectors are implemented in MorphoJ from version 1.05a (Klingenberg 2011).

#### *Modularity of the Braincase and Face*

Many morphological structures are not integrated homogeneously, but are divided into modules, assemblages of parts that are highly integrated internally and relatively independent of other such assemblages (Cheverud 1996; Wagner 1996; Klingenberg 2008, Klingenberg 2013). In such a modular structure, the covariation between subsets of landmarks that correspond to modules is expected to be weaker than the covariation between other partitions of landmarks into subsets that are inconsistent with the modules (in this case, the strong covariation within integrated modules will contribute to covariation between subsets). This expectation can be used directly to develop a criterion for assessing modularity, because modules are expected to be sets of landmarks (or other traits) so that covariation is strong within each set, whereas covariation among different sets is weaker (Klingenberg 2008, 2009). A hypothesis of modularity in morphometric data can therefore be tested by comparing the strength of covariation between the partition of landmarks into

subsets corresponding to the hypothesized modules and alternative partitions into random subsets of landmarks (Klingenberg 2009). The RV coefficient can be used to quantify the covariation between subsets of landmarks. For landmark configurations with relatively few landmarks, such as the one used in this study (Fig. 1), it is feasible to enumerate all partitions of the landmarks into subsets with the same numbers of landmarks as those in the hypothesized modules. It is possible to consider all subdivisions with the appropriate numbers of landmarks or, alternatively, to impose the additional condition that subsets must be spatially contiguous. For this purpose, subsets are defined to be spatially contiguous if the landmarks they contain are linked by the edges of an adjacency graph (Fig. 1; for details, see Klingenberg [2009]). These methods have been used to investigate modularity in insects (Klingenberg 2009; Klingenberg 2010), fish (Kimmel et al. 2012), newts (Ivanović and Kalezić 2010), lizards (Sanger et al. 2012), and mammals (Hallgrímsson et al. 2009; Klingenberg 2009; Drake and Klingenberg 2010; Jamniczky and Hallgrímsson 2011; Jović et al. 2011, 2012; Burgio et al. 2012; Lewton 2012; Sydney et al. 2012), including humans (Bruner et al. 2010; Martínez-Abadías et al. 2012; Wellens et al. 2013). A recent study even has used this approach for assessing modularity in archeological artifacts (González-José and Charlin 2012).

To apply this test of modularity at the level of evolutionary variation, the covariance matrix of independent contrasts can be used in the computations (Drake and Klingenberg 2010). Like the preceding analyses, this test uses the uncentered covariance matrix of independent contrasts to take into account the arbitrary ordering of sister nodes from which the contrasts are computed.

The hypothesis of modularity divides the cranium into an anterior facial module and a posterior neurocranial module (Fig. 1). Such a subdivision has been proposed for developmental reasons: the bones of the face are primarily derived from cranial neural crest, whereas the neurocranium is primarily derived from paraxial mesoderm (Noden and Trainor 2005), and the face appears to harbor more developmental variation than the braincase (Liu et al. 2010). Also, there is a functional subdivision between the two parts, as the face consists substantially of the jaws and parts involved in their movement, whereas the neurocranium houses and protects the brain (Zusi 1993).

## RESULTS

### *Diversification in Shape Space*

The PCA of the variation of skull shapes shows that a large proportion of the variation is contained in relatively few dimensions, with the first three PCs accounting for more than half of the total variance in the sample (Table 1).

A majority of skull shapes in our sample form a dense cluster in shape tangent space, which is surrounded

TABLE 1. PCA of variation among the shapes of species means and independent contrasts, both for the original and size-corrected shape data

	Species means				Contrasts			
	Uncorrected		Size corrected		Uncorrected		Size corrected	
	Eigenvalues	% Total variance	Eigenvalues	% Total variance	Eigenvalues	% Total variance	Eigenvalues	% Total variance
PC1	0.00664	26.6	0.00499	23.1	0.00216	22.6	0.00168	20.4
PC2	0.00426	17.1	0.00360	16.7	0.00167	17.5	0.00136	16.4
PC3	0.00292	11.7	0.00282	13.1	0.00109	11.4	0.00105	12.8
PC4	0.00250	10.0	0.00211	9.8	0.00105	11.0	0.00100	12.1
PC5	0.00201	8.0	0.00186	8.6	0.00084	8.8	0.00056	6.8
PC6	0.00153	6.1	0.00136	6.3	0.00057	6.0	0.00052	6.3
PC7	0.00116	4.7	0.00109	5.0	0.00041	4.3	0.00040	4.8
PC8	0.00079	3.2	0.00079	3.6	0.00040	4.2	0.00038	4.6
PC9	0.00068	2.7	0.00056	2.6	0.00028	3.0	0.00028	3.4

The tabled values are the eigenvalues and percentages of total variance for which each of the first nine PCs accounts.

by a loose scatter of taxa that are more distant from the average shape (Fig. 3). Some extreme points are the woodcock (*Scolopax*), pygmy parrot (*Micropsitta*), rhea (*Rhea*), pelican (*Pelecanus*), and penguin (*Pygoscelis*), among others. Also, there are some groups that are somewhat removed from the main scatter of shapes, especially the owls (including *Aegolius*, *Asio*, *Athene*, *Bubo*, *Otus*, *Strix*, and *Tyto*) and waterfowl (including *Anas*, *Anser*, *Aythya*, *Cygnus*, and *Marmaronetta*).

The shape changes associated with the PCs show some of the main features of cranial variation (Fig. 3). PC1 is associated with dorso-ventral bending of the skull and variation in the relative size of the orbit and relative length of the braincase. PC2 is mostly an axis of variation in the relative length of the anterior part of the face (the ethmoidal region). PC3 features variation between skulls with relatively short and high braincase and relatively large orbits and skulls that are more elongate and have relatively smaller orbits.

The projection of the phylogenetic tree into the PC plots by squared-change parsimony shows extensive crossing of branches and some evidence of relatively long branches between related species (branches that traverse a large proportion of the region occupied by the whole sample; Fig. 3). Nevertheless, some visible clusters that correspond to groups of related taxa, like the owls and waterfowl, suggest that there is some phylogenetic structure in the data as these clades occupy specific regions of shape space.

Mapping the cranial shapes onto the phylogeny using squared-change parsimony yields a tree length of 1.505 (in units of squared Procrustes distance). The permutation test for a phylogenetic signal in the shape data is highly significant ( $P < 0.0001$ ). Similarly, centroid size and log-transformed centroid size also have a highly significant phylogenetic signal (both  $P < 0.0001$ ).

#### Evolutionary Allometry

Because the bird skulls included in this study cover a substantial range of sizes, from hummingbird to

ostrich, allometry is an important potential factor. The multivariate regression of independent contrasts of skull shape on independent contrasts of log-transformed centroid size accounts for 13.0% of the variation in shape and thus indicates that there is clear allometry (Fig. 4). Also, the permutation test indicates that allometry is highly significant statistically ( $P < 0.0001$ ). The shape changes associated with allometry include rearrangement of the upper face and posterior braincase that produce a relatively higher anterior face, smaller orbit, and shorter braincase with increasing skull size (Fig. 4).

Applying the regression vector from the regression with independent contrasts to compute the residual component of variation in taxon averages provides shape scores that are free of the effects of evolutionary allometry (Fig. 5). PC1 of this analysis accounts for slightly less than in the analysis of uncorrected shape, in terms of both the absolute amount (eigenvalue) and the proportion of the total variance (Table 1). The shape features associated with the first three PCs are similar to those of the PCA of the total shape variation (but note that the signs of PC2 and PC3 in Fig. 5 are reversed relative to Fig. 3). The main scatter of skull shapes in this space appears to be somewhat more concentrated (Fig. 5). As in that analysis, however, several taxa are in more remote positions, and these taxa tend to be the same (e.g., *Scolopax*, *Micropsitta*, *Pelecanus*, *Pygoscelis*, as well as the owls and waterfowl). Allometry therefore has a moderate effect on the overall variation of skull shapes, but does not account for the unusual skull shapes of the outlying taxa.

#### Patterns of Variation in Evolutionary Changes

To examine the patterns of evolutionary variation in cranial shape, we examined the covariance matrix of independent contrasts with a PCA (Fig. 6 and Table 1). The shape changes associated with the first two PCs (Fig. 6a) clearly resemble the corresponding PCs in the analysis of species means (Fig. 3; angle between the two

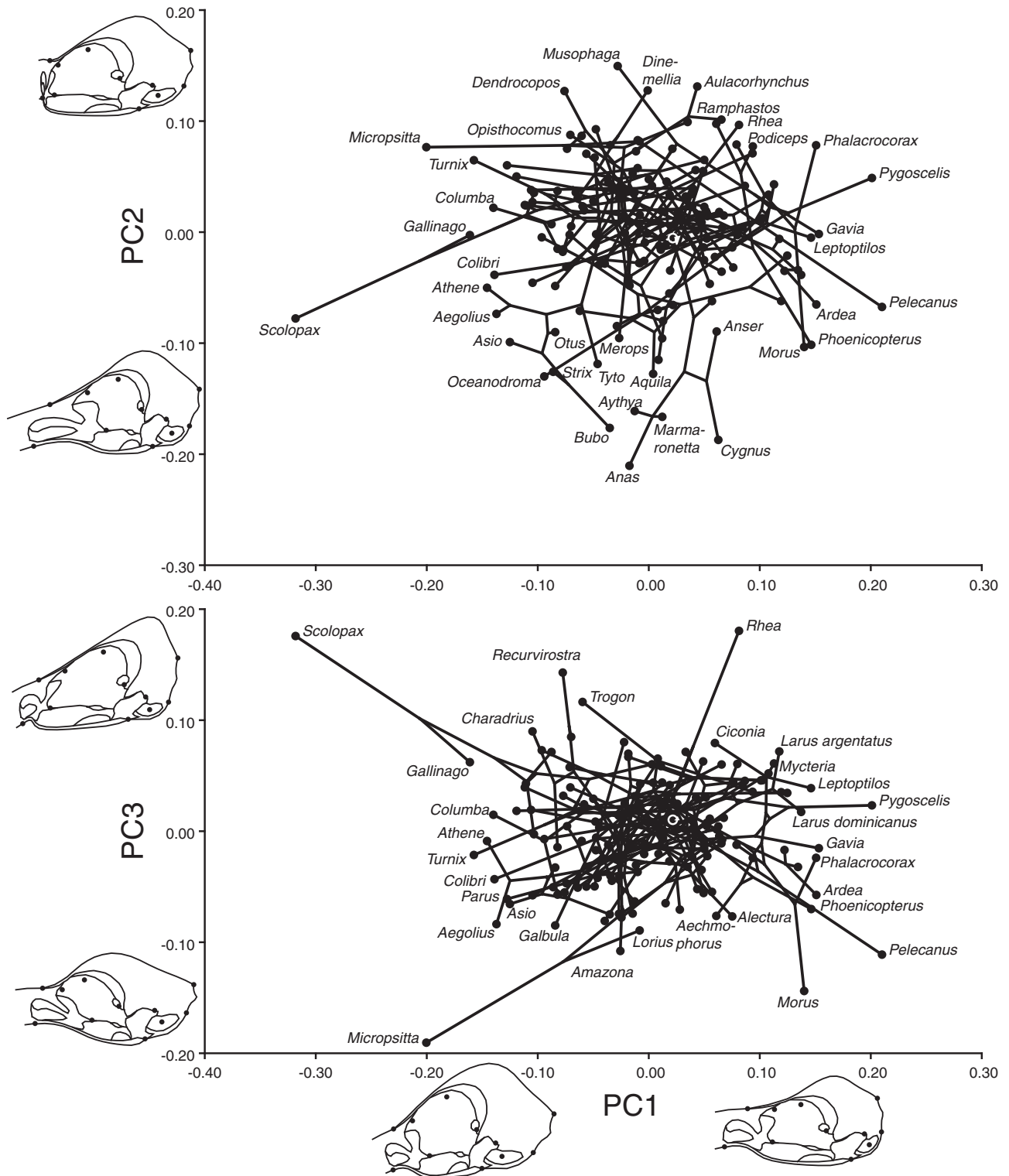


FIGURE 3. Mapping skull shape variation onto the phylogeny of birds. The phylogeny is projected into the shape tangent space by reconstructing shapes at internal nodes by squared-change parsimony and PCs are used to display as much of the variation as possible in few dimensions. Taxa in the periphery of the scatter of points are labeled, as far as space permits. The two diagrams next to each PC axis indicate the skull shapes for a score of  $-0.15$  or  $+0.15$  for the respective PC. Note that the warping of outline diagrams is based on a thin-plate spline for the landmarks (dots) and may therefore not be reliable for positions relatively far from the nearest landmark.

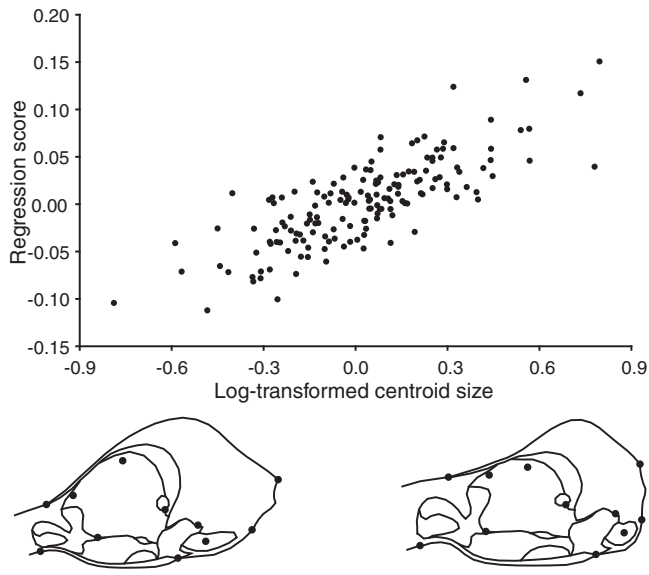


FIGURE 4. Evolutionary allometry of skull shape, based on multivariate regression of independent contrasts of shape on independent contrasts of log-transformed centroid size. The regression score is the shape variable that has the direction of the regression vector in shape space, and its relationship to log-transformed centroid size indicates the strength of allometry. The two drawings show the shapes expected for changes by  $-0.9$  and  $+0.9$  units of log-transformed centroid size from the mean shape (i.e., for the extremes at the left and right of the plot). Because the sign of the contrasts is arbitrary, every data point could equivalently be at a position rotated by  $180^\circ$  about the origin or so that all the contrasts for size are positive (Garland et al. 1992).

PC1s  $19.0^\circ$ ,  $P < 0.0001$ ; angle between the two PC2s  $48.8^\circ$ ,  $P = 0.0022$ ). PC3 differs more clearly and is mostly a dorso-ventral compression or expansion (Fig. 6a); it is most similar to PC4 in the analysis of taxon means and vice versa. The eigenvalues of the independent contrasts are smaller than the corresponding eigenvalues in the PCA for taxon means, but there is a similar distribution of proportions of variation taken up by the different PCs (Table 1).

The shape change for the PC1 of independent contrasts (Fig. 6a) is also similar to the shape change associated with the allometric regression vector (Fig. 4; angle  $22.4^\circ$ ,  $P < 0.0001$ ). As the PC1 takes up 22.6% of the total variation of independent contrasts of shape and the allometric regression accounts for 13.0%, it appears that evolutionary allometry is an important factor in cranial shape diversification, but that other processes must also contribute to the same features of evolutionary shape variation.

To characterize the patterns of evolutionary change without allometric effects, we used a PCA of the residuals from the regression of independent contrasts of shape on the independent contrasts of log-transformed centroid size (Fig. 6b). There is a striking resemblance between the shape change for the PC1 for the size-corrected contrasts (Fig. 6b) and the PC2 of the uncorrected contrasts (Fig. 6a; angle  $16.3^\circ$ ,  $P < 0.00001$ ) and a clear resemblance between the PC2 of size-corrected contrasts and the PC1 of uncorrected contrasts

(Fig. 6a; angle  $41.0^\circ$ ,  $P = 0.00019$ ). The PC3 of size contrasts (Fig. 6b) shows some resemblances with both the PC3 and PC4 of the uncorrected contrasts, so that the correspondence is ambiguous.

#### *Evolutionary Integration of the Face and Braincase*

The analysis of independent contrasts indicates that there is clear evolutionary integration between the face and braincase: the RV coefficient is 0.36, indicating covariation of moderate strength, and the permutation test is highly significant (none of the 250 permutation runs achieved the strength of covariation found in the original data).

For the PLS analysis of independent contrasts without size correction, the first three pairs of PLS axes account for 69.6%, 12.3%, and 8.5% of the total squared covariance between face and braincase. The patterns of covariation show some interesting agreements with the PCAs, but also some clear differences (Fig. 7a). The pair of PLS1 axes (Fig. 7a) is associated with a shape change that is strikingly similar to that of the PC1 (Fig. 6a; angle  $14.8^\circ$ ,  $P < 0.00001$ ), and the shape change for the pair of PLS2 axes resembles that for the PC3 (angle  $43.5^\circ$ ,  $P = 0.00045$ ). The shape change associated with the pair of PLS3 axes, by contrast, has no clear equivalent among the PC axes.

Because allometry is a potential integrating factor, we assess its role in cranial integration by examining the evolutionary covariation between face and braincase after eliminating allometric effects from the independent contrasts of shape. The RV coefficient for the size-corrected contrasts is 0.25 and thus somewhat lower than for the analysis without size correction, but it is still highly significant statistically (none of the 250 permutations matched the strength of covariation in the original data). The first three pairs of PLS axes account for 48.7%, 24.1%, and 13.9% of the total squared covariance between face and braincase. The shape changes of the first two pairs of PLS axes closely correspond to those in the PLS analysis without size correction (Fig. 7; PLS1, angle  $31.2^\circ$ ,  $P < 0.00001$ ; PLS2, angle  $12.1^\circ$ ,  $P < 0.00001$ ), whereas the order is reversed for the PLS3 and PLS4. This also means that the shape change for the pair of PLS1 axes resembles that for the PC2 in the analysis of size-corrected independent contrasts (Fig. 6b; angle  $19.1^\circ$ ,  $P < 0.00001$ ) and the shape change for the PLS2 axes resembles that for the PC3 (angle  $33.9^\circ$ ,  $P < 0.00001$ ).

#### *Evaluating the Hypothesis of Modularity*

Comparing the covariation between the hypothesized facial and neurocranial modules to the covariation between subsets in alternative partitions of the landmarks does not support the hypothesis of modularity. The RV coefficient between the face and braincase, with a value of 0.36, is near the middle of the distribution of RV coefficients for the full enumeration of all 462 partitions of the landmarks into

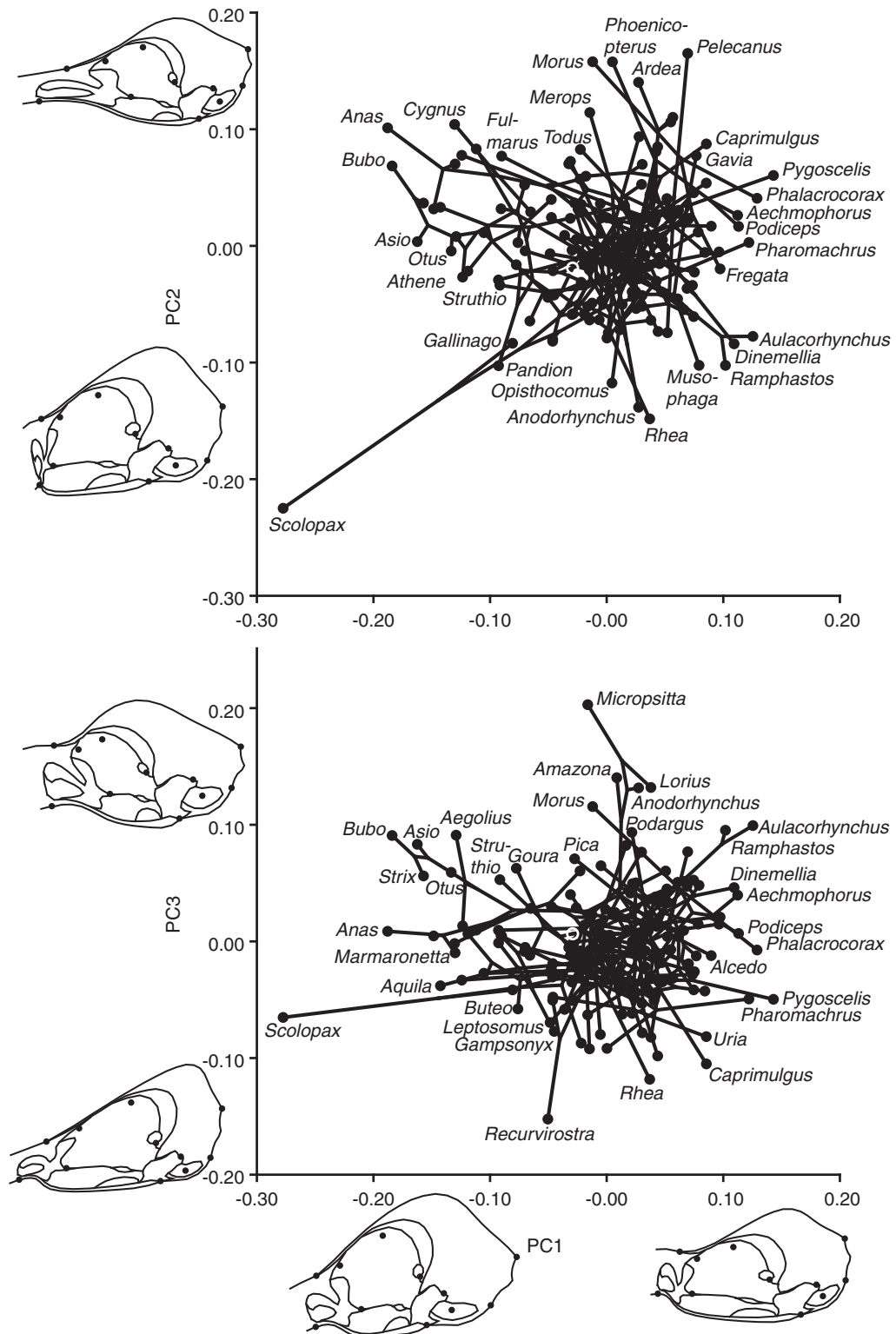


FIGURE 5. Reconstruction of the evolution of avian skull shape in the space of shape after removal of the effects of evolutionary allometry. The ordination of species means is a PCA of the covariance matrix based on residuals computed using the regression vector of independent contrasts, and the phylogenetic tree was projected into this space by squared-change parsimony. The two diagrams next to each PC axis indicate the skull shapes for a score of  $-0.15$  or  $+0.15$  for the respective PC. Taxa in the periphery of the scatter of points are labeled, as far as space permits.

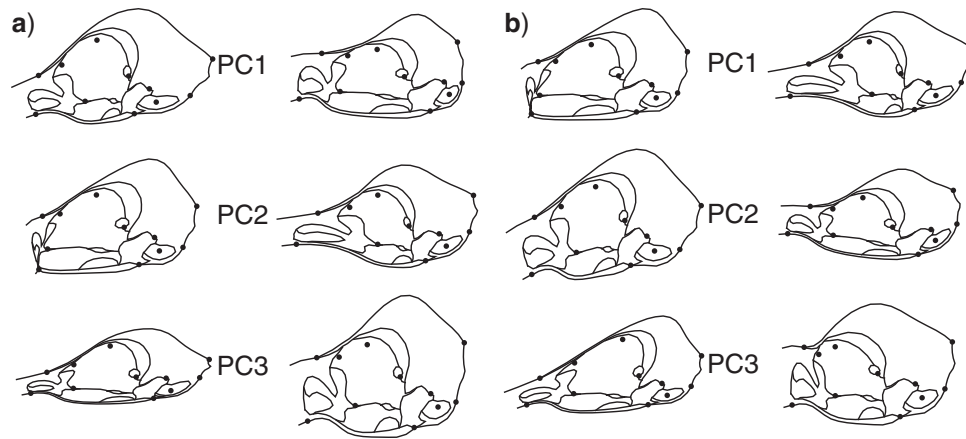


FIGURE 6. Patterns of evolutionary diversification in skull shape: shape changes associated with the PCs of the phylogenetically independent contrasts for shape. a) PCA for independent contrasts for the complete shape variation. b) PCA for the residuals from the regression of independent contrasts of shape on independent contrasts of log-transformed centroid size (Fig. 4). For each PC, the diagrams to the left and right show the shape for a PC score of  $-0.15$  and  $+0.15$ , respectively (these are of similar magnitude as the largest contrasts in the data).

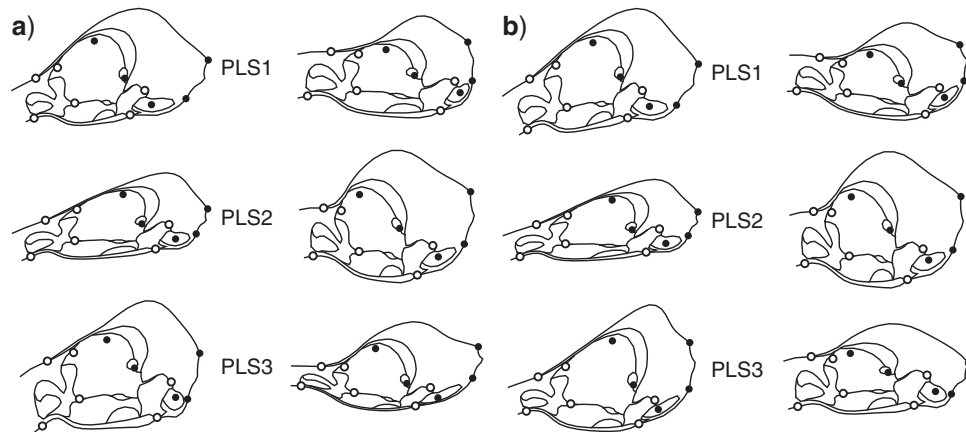


FIGURE 7. Patterns of evolutionary integration between face and braincase: shape changes associated with the PLS axes for phylogenetically independent contrasts. a) PLS analysis for independent contrasts for the complete shape variation. b) PLS analysis for the residuals from the regression of independent contrasts of shape on independent contrasts of log-transformed centroid size (Fig. 4). For each PLS axis, the diagrams to the left and right show the shape for a PLS score of  $-0.15$  and  $+0.15$ , respectively (these are of similar magnitude as the largest contrasts in the data). For each pair of PLS axes, the shape changes for the landmarks of the face (white dots) and the braincase (black dots) are shown in the same diagram.

subsets of five and six landmarks (56.5% of partitions have a lower RV coefficient; Fig. 8a). The same holds if only the 104 spatially contiguous partitions are included in the comparison (49.0% of partitions have a lower RV coefficient; Fig. 8b). These results contradict the expectation that, under the hypothesis of modularity, the covariation between the face and braincase should be weaker than the covariation for alternative partitions of the landmarks.

Because allometry may have integrating effects across the entire skull, it is possible that modularity is more apparent when the effects of allometry are removed from the independent contrasts of shape. The distribution of RV coefficients for size-corrected contrasts of shape (Fig. 8c,d) is shifted to the left relative to the distribution for the uncorrected contrasts (Fig. 8a,b), confirming that allometry does contribute to the overall level of

integration. Nevertheless, the RV coefficient between the face and braincase, with a value of 0.25, is not at the lower end of the distribution, regardless of whether all partitions are considered (17.7% have a lower RV coefficient; Fig. 8c) or whether the comparison is limited to spatially contiguous partitions (14.4% have a lower RV coefficient; Fig. 8d).

## DISCUSSION

This study has used geometric morphometrics in a comparative context to explore the distribution of avian skull shapes in shape space and to investigate evolutionary integration in the skull. The variation of skull shape contains a clear phylogenetic signal, but there are also multiple instances of pronounced

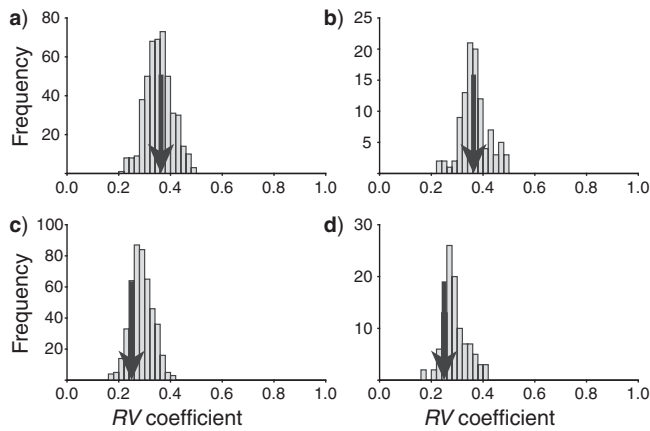


FIGURE 8. Evaluating the hypothesis of evolutionary modularity by comparing the covariation between face and braincase with alternative partitions of the landmarks. a) Covariation of independent contrasts of shape, all possible partitions into sets of six and five landmarks. b) Covariation of independent contrasts of shape, only spatially contiguous partitions. c) Covariation of independent contrasts of shape after size correction, all possible partitions into sets of six and five landmarks. d) Covariation of independent contrasts of shape after size correction, only spatially contiguous partitions. The strength of covariation is quantified as the RV coefficient in the covariance matrix of independent contrasts of shape. The arrows indicate the RV coefficient between the face and braincase, and the histograms represent the distribution of RV coefficients for the alternative partitions into six and five landmarks.

evolutionary divergence among closely related taxa and thus homoplasy. Above all, the analyses showed that there is strong integration of evolutionary changes throughout the skull. Allometry is a contributing factor to this integration, but is not accounting for all the integration in the skull. Finally, there is no evidence that the face and braincase are separate modules, but the skull appears to evolve as a single integrated unit. Here, we evaluate these findings and the methodology.

Given the great variety of skull shapes in birds (e.g., Zusi 1993), it is hardly surprising that they cover a substantial range of shape tangent space (Fig. 3), comparable to other morphometric studies of variation at high taxonomic levels (e.g., Marcus et al. 2000; Wroe and Milne 2007; Drake and Klingenberg 2010; Figueirido et al. 2010, 2013; Friedman 2010; De Esteban-Trivigno 2011a, 2011b; Perez et al. 2011; Álvarez and Perez 2013; Brusatte et al. 2012; Sallan and Friedman 2012; Figueirido et al. 2013) and some examples of remarkable shape diversification at family level or below (e.g., Sidlauskas 2008; Astúa 2009; Cooper et al. 2010; Drake and Klingenberg 2010; Dornburg et al. 2011; Monteiro and Nogueira 2011). Similarly, it is unsurprising that the cranial shape data contain a highly significant phylogenetic signal, according to the permutation test using tree length as the test statistic (Klingenberg and Gidaszewski 2010). This result indicates that phylogenetic methods are needed for investigating the patterns of variation among taxa. It is consistent with earlier studies that found clear taxonomic structure in

skull shapes for specific groups of birds (Brusaferro and Insom 2009; Degrange and Picasso 2010). Despite this phylogenetic signal, however, there is also clear evidence for homoplasy in cranial shape. There is considerable divergence among closely related taxa that reflects the flexibility of the head and beak to evolve, for instance, in response to selection on functional correlates of beak and head morphology (e.g., Grant and Grant 2002; Herrel et al. 2005; van der Meij and Bout 2008; Sievwright and Higuchi 2011). Some instances of convergent evolution in the skull have been pointed out (Zusi 1993; Tokita et al. 2007) and may also contribute to homoplasy in the morphometric data.

The shape changes associated with the PCs of species means (Figs. 3 and 5) and the PCs of independent contrasts (Fig. 6) showed clear correspondence. This is frequently the case in comparative studies, but cannot always be expected, because analyses of variation across the tips of the phylogeny provide estimates of evolutionary patterns that are unbiased, but have higher variance than estimates from comparative methods such as independent contrasts (Rohlf 2006). Analyses that do not take into account the phylogeny may be sensitive to outlying taxa and clades, such as they do occur in this data set (e.g., *Scolopax*, *Pelecanus*, waterfowl, or owls; Figs. 3 and 5).

The patterns of integration revealed by the PCs coincide with patterns of variation, such as various types of bending of the whole skull or of its parts, that have been described earlier by means of various angles and other measurements (reviewed by Zusi 1993) and have been found in previous studies using geometric morphometrics (Marugán-Lobón and Buscalioni 2004, 2006, 2009). The shape changes associated with the various PCs mostly tend to involve relative shifts of landmarks throughout the entire skull (Figs. 3, 5, and 6). An exception to this pattern is the shape change consisting almost exclusively of a shortening or lengthening of the anterior part of the face (PC2 in Figs. 3, 5, and 6a; PC1 in Fig. 6b).

Because allometry produces shape variation that is concentrated in a single dimension of shape space, it is a factor that can contribute substantially to integration throughout an entire structure and it is therefore important to consider allometry in studies of morphological integration (Klingenberg et al. 2001; Rosas and Bastir 2004; Mitteroecker and Bookstein 2007; Klingenberg 2009, 2013). Evolutionary allometry accounts for 13% of the shape variation in independent contrasts. This is comparable to earlier estimates of the proportion of shape variation for which evolutionary allometry accounts (Figueirido et al. 2010; Gonzalez et al. 2011; Perez et al. 2011; Klingenberg et al. 2012) and to similar estimates from intraspecific analyses of static allometry (Rosas and Bastir 2004; Drake and Klingenberg 2008; Klingenberg 2009; Gonzalez et al. 2011; Weisensee and Jantz 2011). Removing the effects of allometry, by using residuals from the regression of shape on size, clearly affects the patterns of overall variation of skull shapes (cf. Figs. 3 vs. 5 and 6a vs. b,

Table 1), patterns of integration between face and braincase (Fig. 7a vs. b), and the strength of covariation (Fig. 8a,b vs. c,d). Although these effects of allometry are noticeable and removing them reduces the RV coefficient between the face and braincase from 0.36 to 0.25, the residuals from the allometric regression still show strong integration throughout the skull. Despite contributing to integration throughout the skull, therefore, allometry is not the main determinant of evolutionary integration.

That shape variation is integrated throughout the skull is further highlighted by the clear correspondence between the PCs of overall cranial variation and PLS axes that characterize covariation between the face and braincase (Figs. 6 and 7). Although the shape changes associated with the PCs and PLS axes are not identical (there is no equivalent to the shape change of PC2 of Fig. 6a and PC1 of Fig. 6b among the PLS axes), there is a clear correspondence between the PCs and PLS axes (cf. Figs. 6 and 7). Because the PLS axes are computed exclusively from information about covariation between the face and braincase and the first few PCs are obtained as those features of shape with the most overall variation, the correspondence between PCs and PLS axes implies that features of integrated evolution in face and braincase are among the dominant features of cranial shape variation. Accordingly, this correspondence of PCs and PLS axes is evidence of overall integration in the whole structure (Klingenberg and Zaklan 2000). Similar correspondence of PCs and PLS axes has been found in other studies of various organisms (Klingenberg and Zaklan 2000; Klingenberg et al. 2001; 2003; Monteiro et al. 2005; Kulemeyer et al. 2009).

PLS analysis has been used to analyze covariation among parts within a configuration in several earlier studies, but mostly at an intraspecific level (Klingenberg and Zaklan 2000; Bookstein et al. 2003; Klingenberg et al. 2003; Bastir and Rosas 2005, 2006; Marugán-Lobón and Buscalioni 2006; Mitteroecker and Bookstein 2008; Kulemeyer et al. 2009; Laffont et al. 2009; Gkantidis and Halazonetis 2011; Jamniczky and Hallgrímsson 2011; Martínez-Abadías et al. 2011; Parsons et al. 2011; Makedonska et al. 2012; Singh et al. 2012; Neaux et al. 2013a; 2013b). Here, we have applied PLS analysis in an explicitly phylogenetic context to investigate evolutionary integration between the face and braincase in birds. Such evolutionary PLS analyses can be carried out using independent contrasts, as in this study, or from covariance matrices estimated with phylogenetic linear models (Rohlf 2001; Revell and Harmon 2008; Blomberg et al. 2012; Meloro and Jones 2012).

Previous morphometric analyses of integration in bird skulls found covariation between the landmarks used here and a series of endocranial measurements (Marugán-Lobón and Buscalioni 2006). This indicates that evolutionary changes in external and internal features of the skull covary, even though the physical separation of internal and external surfaces that is associated with cranial pneumatization in birds should provide a degree of independence between internal and

external traits of the skull (Zusi 1993). Clear integration of skull shape was also found in a study that used similar methods to investigate integration between the beak and skull (including most of the facial region; Fig. 1) in several species of corvids (Kulemeyer et al. 2009). Given the importance of cranial kinesis for the movements of the beak in birds (Zusi 1993; Bout and Zweers 2001; Meekangvan et al. 2006; Dawson et al. 2011), it might also be expected that variation in the face—containing structures such as the base of the beak, jugal bar, and quadrate bone, which are involved in movements relative to the braincase—would evolve as a separate unit from the braincase. Our results indicate that this is not the case, but that the entire skull appears to evolve as a coordinated unit.

Such strong cranial integration is consistent with the hypothesis that heterochrony plays a strong role in the evolution of bird skulls. For instance, morphometric analyses suggest that bird skulls are pedomorphic by comparison with other theropods (Bhullar et al. 2012). Some of the shape features found in the shape changes associated with the PC1 and allometry in this study (Figs. 3 and 4) qualitatively resemble the main shape features associated with ontogenetic change in a Darwin's finch (Genbrugge et al. 2011) and in theropods (Bhullar et al. 2012). If such ontogenetic scaling affects the skull as a whole and accounts for a substantial portion of cranial evolution, integration of evolutionary changes is expected to result (e.g., Mitteroecker et al. 2005; Drake 2011). This reasoning is further complicated, however, because avian ontogenetic trajectories have been shown to be clearly nonlinear, with abrupt changes of direction associated with hatching or fledging (Cane 1993; Genbrugge et al. 2011). Because information on ontogenetic trajectories in birds is scarce, it is difficult to gauge the possible role of such nonlinear trajectories and scaling in avian evolution.

The data considered in this study do not support the hypothesis that the face and braincase are separate evolutionary modules (Fig. 8). The hypothesis predicts that the partition of the landmarks into subsets corresponding to the face and braincase should result in a weaker covariation between subsets than alternative partitions. In our data of independent contrasts for skull shape, however, the covariation between face and braincase is stronger than a substantial proportion of other partitions. The correction for the effects of allometry reduces this proportion to a degree (Fig. 8c,d), as is consistent with the expectation that allometry contributes to overall integration in the skull. The rejection of the hypothesis of modularity is consistent with the results of PCA and PLS analyses, which also point to strong integration throughout the skull. This differs from findings in some mammals, where modularity of the face and braincase was found with the same methods in intra- and interspecific analyses (Drake and Klingenberg 2010; Jojić et al. 2011; Sydney et al. 2012), but full integration throughout the skull was also found in a study of humans (Martínez-Abadías et al. 2012; but

see also Wellens et al. 2013) and another study rejected several hypotheses of modularity for the skull of mice (Hallgrímsson et al. 2009). In a wide range of vertebrates, various hypotheses of intraspecific modularity in the skull and mandible have been tested and have produced heterogeneous results (Klingenberg 2009; Ivanović and Kalezić 2010; Burgio et al. 2012; Jojić et al. 2012; Kimmel et al. 2012; Sanger et al. 2012; Klingenberg 2013). With different methods, various patterns of modularity were found within species in mammals using geometric morphometrics (Goswami 2006a, 2006b, 2007) and traditional morphometrics (Cheverud 1982a, 1995; Porto et al. 2009; Shirai and Marroig 2010). Comparisons of results among these studies are difficult because of the different morphometric methods and concepts of modularity and integration they use. However, the only study that made a direct comparison found that the methods used here and traditional morphometrics produced compatible results, suggesting that comparisons are possible (Jojić et al. 2012). Comparisons between studies across vertebrate classes are also problematic for anatomical reasons: for instance, the premaxilla of birds, by comparison to mammals, is extraordinarily variable because of the great variability of the beak in birds, and the quadrate bone, which is a prominent element of the articulation of jaws and jugal bar in birds, is homologous to one of the middle ear ossicles, the incus, in mammals. Because of such differences in the anatomical structure of the skull, it may be impossible to find landmarks in one group that are homologues of the landmarks in another group, and even if homologous landmarks are available, patterns of integration and modularity may not be comparable if differences in the organization of skulls fundamentally alter the anatomical and functional context. To assess patterns of evolutionary modularity and their relation to modularity and integration within taxa, further studies in a phylogenetic comparative context are necessary.

Previous discussions of comparative methods have mostly emphasized regression analysis (Felsenstein 1985; Harvey and Pagel 1991; Martins and Hansen 1997; Rohlf 2001, 2006; Blomberg et al. 2012). We used multivariate regression of independent contrasts to assess evolutionary allometry and correct for its effects (Revell 2009; Figueirido et al. 2010; Perez et al. 2011; Klingenberg et al. 2012). Here, we show that a range of other multivariate methods can also be used in a comparative context to understand evolutionary changes of shape: PCA (Revell 2009, with modifications for geometric morphometrics), PLS, and tests of modularity. As in other applications of geometric morphometrics, some adjustments may be needed, but these adjustments can be made with independent contrasts in a similar way as they are firmly established in other contexts such as fluctuating asymmetry (e.g., including a Procrustes fit in the algorithm of the permutation test for covariation within a configuration of landmarks; Klingenberg et al. 2003). The tools of geometric morphometrics, in such a comparative context, will be able to answer many specific questions

about evolutionary diversification of shape and its history.

Throughout this article, we have used independent contrasts as the method for taking into account the phylogenetic nature of the comparative data. Other methods are available and can also be used in the context of geometric morphometrics. In particular, PGLS methods have been widely used and multivariate versions are available (e.g., Martins and Hansen 1997; Rohlf 2001; Revell and Harmon 2008). These methods are mathematically equivalent to independent contrasts and, with the same evolutionary model, provide equivalent results (Rohlf 2001; Garland et al. 2005; Blomberg et al. 2012). In both approaches, a range of evolutionary models can be implemented by adjusting the branch lengths in the phylogeny (e.g., punctuated equilibria can be modeled by specifying zero-length branches for evolutionary lineages exhibiting stasis; Felsenstein 2004).

Perhaps the main difference between the different approaches is in what constitutes the units of analysis. Independent contrasts are weighted differences between the phenotypes of sister nodes in the phylogeny (either directly observed in terminal taxa or locally reconstructed from the phenotypes of descendants for internal nodes), and therefore explicitly focus on evolutionary change. By contrast, although phylogenetic interdependence is taken into account statistically in PGLS, the units of the analysis are the observed taxa. Because the appropriate target for explanations in evolutionary biology is evolutionary change and not the states of taxa (O'Hara 1988), it is at least a didactic advantage of independent contrasts that they explicitly focus on evolutionary change as the unit of analysis and not the states of taxa as in PGLS. A further advantage of independent contrasts is that they can be treated like other shape differences (e.g., fluctuating asymmetry) and therefore can be accommodated in standard morphometric software with only minor modifications. Independent contrasts are therefore a convenient and natural way to use all the standard tools of geometric morphometrics in the context of phylogenetic comparative approaches.

Because the concepts of morphological integration and modularity apply at multiple levels from within-organism variation to phylogenetic diversification (Breuker et al. 2006; Klingenberg 2008, 2010, 2013), a particularly promising application for these morphometric tools will be in coordinated analyses of variation at multiple levels: fluctuating asymmetry within individuals, phenotypic and genetic variation among individuals within taxa, and evolutionary variation among taxa. Some studies have been conducted that combine within-taxon analyses and phylogenetic comparative analyses (Drake and Klingenberg 2010; Gonzalez et al. 2011; Klingenberg et al. 2012; Klingenberg 2013). Such multilevel analyses are promising to advance our understanding of the interface between micro- and macroevolution and will allow inferences on the evolutionary processes involved in the diversification of

major clades (Monteiro et al. 2005; Hunt 2007; Sidlauskas 2008; Klingenberg 2010).

#### SUPPLEMENTARY MATERIAL

Supplementary material, consisting of the data and phylogeny files, can be found in the Dryad data repository at <http://datadryad.org>, doi:10.5061/dryad.787c0.

#### FUNDING

Funding for this study was provided through grants from AMNH Collection Study Grants, EU Synthesys and Project DGCYT CGL2009\_11838 BTE, from the Ministerio de Economía y Competitividad, Gobierno de España (to J.M.L.).

#### ACKNOWLEDGMENTS

The authors thank Paul Sweet (AMNH), Sylke Frahnert (MFN-Berlin), Francisco Pastor (UVA), and Josefina Berreiro (MNCN), for granting access and help with the bird collections at their institutions. They also thank members of the Klingenberg lab, Joe Felsenstein, Benedikt Hallgrímsson, Norm MacLeod, and three anonymous reviewers for helpful and critical comments on earlier versions.

#### REFERENCES

- Acosta Hospitaleche C., Tambussi C. 2006. Skull morphometry of *Pygoscelis* (Sphenisciformes): inter and intraspecific variations. *Polar Biol.* 29:728–734.
- Adams D.C., Nistri A. 2010. Ontogenetic convergence and evolution of foot morphology in European cave salamanders (Family: Plethodontidae). *BMC Evol. Biol.* 10:216.
- Adams D.C., Rohlf F.J. 2000. Ecological character displacement in *Plethodon*: biomechanical differences found from a geometric morphometric study. *Proc. Natl Acad. Sci. U. S. A.* 97:4106–4111.
- Álvarez A., Perez S.I. 2013. Two- versus three-dimensional morphometric approaches in macroevolution: insight from the mandible of caviomorph rodents. *Evol. Biol.* 40:150–157.
- Arthur W. 2001. Developmental drive: an important determinant of the direction of phenotypic evolution. *Evol. Dev.* 3:271–278.
- Astúa D. 2009. Evolution of scapular size and shape in didelphid marsupials (Didelphimorphia: Didelphidae). *Evolution* 63:2438–2456.
- Baker A.J., Pereira S.L., Paton T.A. 2007. Phylogenetic relationships and divergence times of Charadriiformes genera: multigene evidence for the Cretaceous origin of at least 14 clades of shorebirds. *Biol. Lett.* 3:205–209.
- Barker F.K., Lanyon S.M. 2000. The impact of parsimony weighting schemes on inferred relationships among toucans and Neotropical barbets (Aves: Piciformes). *Mol. Phylogenet. Evol.* 15:215–234.
- Bastir M. 2008. A systems-model for the morphological analysis of integration and modularity in human craniofacial evolution. *J. Anthropol. Sci.* 86:37–58.
- Bastir M., Rosas A. 2005. Hierarchical nature of morphological integration and modularity in the human posterior face. *Am. J. Phys. Anthropol.* 128:26–34.
- Bastir M., Rosas A. 2006. Correlated variation between the lateral basicranium and the face: a geometric morphometric study in different human groups. *Arch. Oral Biol.* 51:814–824.
- Bastir M., Rosas A., Gunz P., Peña-Melian A., Manzi G., Harvati K., Kruszynski R., Stringer C.B., Hublin J.-J. 2011. Evolution of the base of the brain in highly encephalized human species. *Nat. Commun.* 2:588.
- Benz B.W., Robbins M.B., Peterson A.T. 2006. Evolutionary history of woodpeckers and allies (Aves: Picidae): placing key taxa on the phylogenetic tree. *Mol. Phylogenet. Evol.* 40:389–399.
- Bhullar B.-A.S., Marugán-Lobón J., Racimo F., Bever G.S., Rowe T.B., Norell M.A., Abzhanov A. 2012. Birds have pedomorphic dinosaur skulls. *Nature* 487:223–226.
- Blomberg S.P., Lefevre J.G., Wells J.A., Waterhouse M. 2012. Independent contrasts and PGLS regression estimators are equivalent. *Syst. Biol.* 61:382–391.
- Bookstein F.L. 1991. Morphometric tools for landmark data: geometry and biology. Cambridge: Cambridge University Press.
- Bookstein F.L., Chernoff B., Elder R.L., Humphries J.M. Jr., Smith G.R., Strauss R.E. 1985. Morphometrics in evolutionary biology: the geometry of size and shape change, with examples from fishes. Philadelphia (PA): Academy of Natural Sciences of Philadelphia.
- Bookstein F.L., Gunz P., Mitteroecker P., Prossinger H., Schaefer K., Seidler H. 2003. Cranial integration in *Homo*: singular warps analysis of the midsagittal plane in ontogeny and evolution. *J. Hum. Evol.* 44:167–187.
- Bout R.G., Zweers G.A. 2001. The role of cranial kinesis in birds. *Comp. Biochem. Physiol. Part A Mol. Integr. Physiol.* 131:197–205.
- Breuker C.J., Debat V., Klingenberg C.P. 2006. Functional evo-devo. *Trends Ecol. Evol.* 21:488–492.
- Bruner E., Martin-Loeches M., Colom R. 2010. Human midsagittal brain shape variation: patterns, allometry and integration. *J. Anat.* 216:589–599.
- Brusaferro A., Insom E. 2009. Morphometric analysis of the kingfisher cranium (AVES). *Ital. J. Zool.* 76:53–63.
- Brusatte S.L., Sakamoto M., Montanari S., Harcourt Smith W.E.H. 2012. The evolution of cranial form and function in theropod dinosaurs: insights from geometric morphometrics. *J. Evol. Biol.* 25:365–377.
- Burgio G., Baylac M., Heyer E., Montagutelli X. 2012. Exploration of the genetic organization of morphological modularity on the mouse mandible using a set of interspecific recombinant congenic strains between C57BL/6 and mice of the *Mus spretus* species. *G3 (Bethesda)* 2:1257–1268.
- Cane W.P. 1993. The ontogeny of postcranial integration in the common tern, *Sterna hirundo*. *Evolution* 47:1138–1151.
- Chamero B., Buscalioni Á.D., Marugán-Lobón J. 2013. Pectoral girdle and forelimb variation in extant Crocodylia: the coracoid-humerus pair as an evolutionary module. *Biol. J. Linn. Soc.* 108:600–618.
- Chernoff B., Magwene P.M. 1999. Afterword—morphological integration: forty years later. In: Olson E.C., Miller R.L. Morphological integration. Chicago (IL): University of Chicago Press. p. 319–353.
- Cheverud J.M. 1982a. Phenotypic, genetic, and environmental morphological integration in the cranium. *Evolution* 36:499–516.
- Cheverud J.M. 1982b. Relationships among ontogenetic, static, and evolutionary allometry. *Am. J. Phys. Anthropol.* 59:139–149.
- Cheverud J.M. 1995. Morphological integration in the saddle-back tamarin (*Saguinus fuscicollis*) cranium. *Am. Nat.* 145:63–89.
- Cheverud J.M. 1996. Developmental integration and the evolution of pleiotropy. *Amer. Zool.* 36:44–50.
- Cock A.G. 1966. Genetical aspects of metrical growth and form in animals. *Q. Rev. Biol.* 41:131–190.
- Cooper W.J., Parsons K.J., McIntyre A., Kern B., McGee-Moore A., Albertson R.C. 2010. Benthic-pelagic divergence of cichlid feeding architecture was prodigious and consistent during multiple adaptive radiations within African rift-lakes. *PLoS One* 5:e9551.
- Corti M., Rohlf F.J. 2001. Chromosomal speciation and phenotypic evolution in the house mouse. *Biol. J. Linn. Soc.* 73:99–112.
- Dawson M.M., Metzger K.A., Baier D.B., Brainerd E.L. 2011. Kinematics of the quadrate bone during feeding in mallard ducks. *J. Exp. Biol.* 214:2036–2046.

- De Esteban-Trivigno S. 2011a. Buscando patrones ecomorfológicos comunes entre ungulados actuales y xenartros extintos. *Ameghiniana* 48:189–209.
- De Esteban-Trivigno S. 2011b. Ecomorfología de xenartros extintos: análisis de la mandíbula con métodos de morfometría geométrica. *Ameghiniana* 48:381–398.
- Degrange F.J., Picasso M.B.J. 2010. Geometric morphometrics of the skull of Tinamidae (Aves, Palaeognathae). *Zoology (Jena)* 113:334–338.
- Dornburg A., Sidlauskas B., Santini F., Sorenson L., Near T.J., Alfaro M.E. 2011. The influence of an innovative strategy on the phenotypic diversification of triggerfish (family: Balistidae). *Evolution* 65:1912–1926.
- Drake A.G. 2011. Dispelling dog dogma: an investigation of heterochrony in dogs using 3D geometric morphometric analysis of skull shape. *Evol. Dev.* 13:204–213.
- Drake A.G., Klingenberg C.P. 2008. The pace of morphological change: historical transformation of skull shape in St. Bernard dogs. *Proc. R. Soc. Lond. B Biol. Sci.* 275:71–76.
- Drake A.G., Klingenberg C.P. 2010. Large-scale diversification of skull shape in domestic dogs: disparity and modularity. *Am. Nat.* 175:289–301.
- Dryden I.L., Mardia K.V. 1998. *Statistical shape analysis*. Chichester: Wiley.
- Eo S.H., Bininda-Emonds O.R.P., Carroll J.P. 2009. A phylogenetic supertree of the fowls (Galloanserae, Aves). *Zool. Scr.* 38:465–481.
- Escoufier Y. 1973. Le traitement des variables vectorielles. *Biometrics* 29:751–760.
- Fain M.G., Krajewski C., Houde P. 2007. Phylogeny of “core Gruiformes” (Aves: Grues) and resolution of the Limpkin–Sungrebe problem. *Mol. Phylogenet. Evol.* 43:515–529.
- Felsenstein J. 1985. Phylogenies and the comparative method. *Am. Nat.* 125:1–15.
- Felsenstein J. 1988. Phylogenies and quantitative characters. *Annu. Rev. Ecol. Syst.* 19:455–471.
- Felsenstein J. 2004. *Inferring phylogenies*. Sunderland (MA): Sinauer Associates.
- Felsenstein J. 2008. Comparative methods with sampling error and within-species variation: contrasts revisited and revised. *Am. Nat.* 171:713–725.
- Figueirido B., Serrano-Alarcón F.J., Slater G.J., Palmqvist P. 2010. Shape at the cross-roads: homoplasy and history in the evolution of the carnivoran skull towards herbivory. *J. Evol. Biol.* 23:2579–2594.
- Figueirido B., Tseng Z.J., Martín-Serra A. 2013. Skull shape evolution in durophagous carnivorans. *Evolution*. doi: 10.1111/evo.12059.
- Fortuny J., Marcé Nogué J., De Esteban-Trivigno S., Gil L., Galobart À. 2011. Temnospondyli bite club: ecomorphological patterns of the most diverse group of early tetrapods. *J. Evol. Biol.* 24:2040–2054.
- Friedman M. 2010. Explosive morphological diversification of spiny-finned teleost fishes in the aftermath of the end-Cretaceous extinction. *Proc. R. Soc. Lond. B Biol. Sci.* 277:1675–1683.
- García Z., Sarmiento C.E. 2012. Relationship between body size and flying-related structures in Neotropical social wasps (Polistinae, Vespidae, Hymenoptera). *Zoomorphology (Berl.)* 131:25–35.
- Garland T. Jr., Bennett A.F., Rezende E.L. 2005. Phylogenetic approaches in comparative physiology. *J. Exp. Biol.* 208:3015–3035.
- Garland T. Jr., Harvey P.H., Ives A.R. 1992. Procedures for the analysis of comparative data using phylogenetically independent contrasts. *Syst. Biol.* 41:18–32.
- Garland T. Jr., Midford P.E., Ives A.R. 1999. An introduction to phylogenetically based statistical methods with a new method for confidence intervals on ancestral values. *Am. Zool.* 39:374–388.
- Genbrugge A., Heyde A.-S., Adriaens D., Boone M., Van Hoorebeke L., Dirckx J., Aerts P., Podos J., Herrel A. 2011. Ontogeny of the cranial skeleton in a Darwin’s finch (*Geospiza fortis*). *J. Anat.* 219:115–131.
- Gidaszewski N.A., Baylac M., Klingenberg C.P. 2009. Evolution of sexual dimorphism of wing shape in the *Drosophila melanogaster* subgroup. *BMC Evol. Biol.* 9:110.
- Gkantidis N., Halazonetis D.J. 2011. Morphological integration between the cranial base and the face in children and adults. *J. Anat.* 218:426–438.
- Gómez-Robles A., Martín-Torres M., Bermúdez de Castro J.M., Prado-Simón L., Arsuaga J.L. 2011. A geometric morphometric analysis of hominin upper premolars. Shape variation and morphological integration. *J. Hum. Evol.* 61:688–702.
- Gómez-Robles A., Polly P.D. 2012. Morphological integration in the hominin dentition: evolutionary, developmental, and functional factors. *Evolution* 66:1024–1043.
- Gonzalez P.N., Kristensen E., Morck D.W., Boyd S.K., Hallgrímsson B. 2013. Effects of growth hormone on the ontogenetic allometry of craniofacial bones. *Evol. Dev.* 15:133–145.
- Gonzalez P.N., Perez S.I., Bernal V. 2010. Ontogeny of robusticity of craniofacial traits in modern humans: a study of South American populations. *Am. J. Phys. Anthropol.* 142:367–379.
- Gonzalez P.N., Perez S.I., Bernal V. 2011. Ontogenetic allometry and cranial shape diversification among human populations from South America. *Anat. Rec.* 294:1864–1874.
- González-José R., Charlin J. 2012. Relative importance of modularity and other morphological attributes of different types of lithic point weapons: assessing functional variations. *PLoS One* 7:e48009.
- Good P. 2000. *Permutation tests: a practical guide to resampling methods for testing hypotheses*. 2nd ed. New York: Springer.
- Goodall C.R. 1991. Procrustes methods in the statistical analysis of shape. *J. R. Statist. Soc. B* 53:285–339.
- Goswami A. 2006a. Cranial modularity shifts during mammalian evolution. *Am. Nat.* 168:270–280.
- Goswami A. 2006b. Morphological integration in the carnivoran skull. *Evolution* 60:169–183.
- Goswami A. 2007. Phylogeny, diet and cranial integration in australodelphian marsupials. *PLoS One* 2:e995.
- Goswami A., Polly P.D. 2010. Methods for studying morphological integration and modularity. In: Alroy J., Hunt G., editors. *Quantitative methods in paleobiology*. Ithaca (NY): Paleontological Society. p. 213–243.
- Gould S.J. 1966. Allometry and size in ontogeny and phylogeny. *Biol. Rev.* 41:587–640.
- Gould S.J. 1989. A developmental constraint in *Cerion*, with comments on the definition and interpretation of constraint in evolution. *Evolution* 43:516–539.
- Grant P.R., Grant B.R. 2002. Unpredictable evolution in a 30-year study of Darwin’s finches. *Science* 296:707–711.
- Haber A. 2011. A comparative analysis of integration indices. *Evol. Biol.* 38:476–488.
- Hackett S.J., Kimball R.T., Reddy S., Bowie R.C.K., Braun E.L., Braun M.J., Chojnowski J.L., Cox W.A., Han K.-L., Harshman J., Huddleston C.J., Marks B.D., Miglia K.J., Moore W.S., Sheldon F.H., Steadman D.W., Witt C.C., Yuri T. 2008. A phylogenomic study of birds reveals their evolutionary history. *Science* 320:1763–1767.
- Hallgrímsson B., Jamniczky H.A., Young N.M., Rolian C., Parsons T.E., Boughner J.C., Marcucio R.S. 2009. Deciphering the palimpsest: studying the relationship between morphological integration and phenotypic covariation. *Evol. Biol.* 36:355–376.
- Harvey P.H., Pagel M.D. 1991. *The comparative method in evolutionary biology*. Oxford: Oxford University Press.
- Hautier L., Lebrun R., Cox P.G. 2012. Patterns of covariation in the masticatory apparatus of hystricognathous rodents: implications for evolution and diversification. *J. Morphol.* 273:1319–1337.
- Herrel A., Podos J., Huber S.K., Hendry A.P. 2005. Evolution of bite force in Darwin’s finches: a key role for head width. *J. Evol. Biol.* 18:669–675.
- Herrel A., Soons J., Aerts P., Dirckx J., Boone M., Jacobs P., Adriaens D., Podos J. 2010. Adaptation and function of the bills of Darwin’s finches: divergence by feeding type and sex. *Emu* 110:39–47.
- Hunt G. 2007. Evolutionary divergence in directions of high phenotypic variance in the ostracode genus *Poseidonamicus*. *Evolution* 61:1560–1576.
- Ivanović A., Kalezić M.L. 2010. Testing the hypothesis of morphological integration on a skull of a vertebrate with a biphasic life cycle: a case study of the alpine newt. *J. Exp. Zool. B Mol. Dev. Evol.* 314:527–538.
- Ives A.R., Midford P.E., Garland T. Jr. 2007. Within-species variation and measurement error in phylogenetic comparative methods. *Syst. Biol.* 56:252–270.

- Jamniczky H.A., Hallgrímsson B. 2011. Modularity in the skull and cranial vasculature of laboratory mice: implications for the evolution of complex phenotypes. *Evol. Dev.* 13:28–37.
- Jetz W., Thomas G.H., Joy J.B., Hartmann K., Mooers A.Ø. 2012. The global diversity of birds in space and time. *Nature* 491: 444–448.
- Jojić V., Blagojević J., Vujošević M. 2011. B chromosomes and cranial variability in yellow-necked field mice (*Apodemus flavicollis*). *J. Mammal.* 92:396–406.
- Jojić V., Blagojević J., Vujošević M. 2012. Two-module organization of the mandible in the yellow-necked mouse: a comparison between two different morphometric approaches. *J. Evol. Biol.* 25: 2489–2500.
- Jolliffe I.T. 2002. Principal component analysis. 2nd ed. New York: Springer-Verlag.
- Jönsson K.A., Fjeldså J. 2006. A phylogenetic supertree of oscine passerine birds (Aves: Passeri). *Zool. Scr.* 35:149–186.
- Kimmel C.B., Hohenlohe P.A., Ullmann B., Currey M., Cresko W.A. 2012. Developmental dissociation in morphological evolution of the stickleback opercle. *Evol. Dev.* 14:326–337.
- Kleinteich T., Maddin H.C., Herzen J., Beckmann F., Summers A.P. 2012. Is solid always best? Cranial performance in solid and fenestrated caecilian skulls. *J. Exp. Biol.* 215:833–844.
- Klingenberg C.P. 1996. Multivariate allometry. In: Marcus L.F., Corti M., Loy A., Naylor G.J.P., Slice D.E., editors. *Advances in morphometrics*. New York: Plenum Press. p. 23–49.
- Klingenberg C.P. 2008. Morphological integration and developmental modularity. *Annu. Rev. Ecol. Evol. Syst.* 39:115–132.
- Klingenberg C.P. 2009. Morphometric integration and modularity in configurations of landmarks: tools for evaluating a-priori hypotheses. *Evol. Dev.* 11:405–421.
- Klingenberg C.P. 2010. Evolution and development of shape: integrating quantitative approaches. *Nat. Rev. Genet.* 11:623–635.
- Klingenberg C.P. 2011. MorphoJ: an integrated software package for geometric morphometrics. *Mol. Ecol. Resour.* 11:353–357.
- Klingenberg C.P. 2013. Cranial integration and modularity: insights into evolution and development from morphometric data. *Hystrix* 24 (in press) doi: 10.4404/hystrix-24.1-6367.
- Klingenberg C.P., Badyaev A.V., Sowry S.M., Beckwith N.J. 2001. Inferring developmental modularity from morphological integration: analysis of individual variation and asymmetry in bumblebee wings. *Am. Nat.* 157:11–23.
- Klingenberg C.P., Debat V., Roff D.A. 2010. Quantitative genetics of shape in cricket wings: developmental integration in a functional structure. *Evolution* 64:2935–2951.
- Klingenberg C.P., Duttke S., Whelan S., Kim M. 2012. Developmental plasticity, morphological variation and evolvability: a multilevel analysis of morphometric integration in the shape of compound leaves. *J. Evol. Biol.* 25:115–129.
- Klingenberg C.P., Ekau W. 1996. A combined morphometric and phylogenetic analysis of an ecomorphological trend: pelagization in Antarctic fishes (Perciformes: Nototheniidae). *Biol. J. Linn. Soc.* 59:143–177.
- Klingenberg C.P., Gidaszewski N.A. 2010. Testing and quantifying phylogenetic signals and homoplasy in morphometric data. *Syst. Biol.* 59:245–261.
- Klingenberg C.P., McIntyre G.S. 1998. Geometric morphometrics of developmental instability: analyzing patterns of fluctuating asymmetry with Procrustes methods. *Evolution* 52:1363–1375.
- Klingenberg C.P., Mebus K., Auffray J.-C. 2003. Developmental integration in a complex morphological structure: how distinct are the modules in the mouse mandible? *Evol. Dev.* 5:522–531.
- Klingenberg C.P., Zaklan S.D. 2000. Morphological integration between developmental compartments in the *Drosophila* wing. *Evolution* 54:1273–1285.
- Klingenberg C.P., Zimmermann M. 1992. Static, ontogenetic, and evolutionary allometry: a multivariate comparison in nine species of water striders. *Am. Nat.* 140:601–620.
- Kulemeyer C., Asbahr K., Gunz P., Frahnert S., Bairlein F. 2009. Functional morphology and integration of corvid skulls—a 3D geometric morphometric approach. *Front. Zool.* 6:2.
- Laffont R., Renvoisé E., Navarro N., Alibert P., Montuire S. 2009. Morphological modularity and assessment of developmental processes within the vole dental row (*Microtus arvalis*, Arvicolinae, Rodentia). *Evol. Dev.* 11:302–311.
- Lerner H.R.L., Mindell D.P. 2005. Phylogeny of eagles, Old World vultures, and other Accipitridae based on nuclear and mitochondrial DNA. *Mol. Phylogenet. Evol.* 37:327–346.
- Lewton K.L. 2012. Evolvability of the primate pelvic girdle. *Evol. Biol.* 39:126–139.
- Li S. 2011. Concise formulas for the area and volume of a hyperspherical cap. *Asian J. Math. Statist.* 4:66–70.
- Linde M., Palmer M., Gómez-Zurita J. 2004. Differential correlates of diet and phylogeny on the shape of the premaxilla and anterior tooth in sparid fishes (Perciformes: Sparidae). *J. Evol. Biol.* 17: 941–952.
- Liu B., Rooker S.M., Helms J.A. 2010. Molecular control of facial morphology. *Semin. Cell Dev. Biol.* 21:309–313.
- Loy A., Cataudella S., Corti M. 1996. Shape changes during the growth of the sea bass, *Dicentrarchus labrax* (Teleostea: Perciformes), in relation to different rearing conditions. In: Marcus L.F., Corti M., Loy A., Naylor G.J.P., Slice D.E., editors. *Advances in morphometrics*. New York: Plenum Press. p. 399–405.
- Loy A., Mariani L., Bertelletti M., Tunesi L. 1998. Visualizing allometry: geometric morphometrics in the study of shape changes in the early stages of the two-banded sea bream, *Diplodus vulgaris* (Perciformes, Sparidae). *J. Morphol.* 237:137–146.
- Maddison W.P. 1991. Squared-change parsimony reconstructions of ancestral states for continuous-valued characters on a phylogenetic tree. *Syst. Zool.* 40:304–314.
- Maddison W.P., Maddison D.R. 2011. Mesquite: a modular system for evolutionary analysis. Version 2.75. <http://mesquiteproject.org> (last accessed May 5, 2013).
- Makedonska J., Wright B.W., Strait D.S. 2012. The effect of dietary adaptation on cranial morphological integration in capuchins (order Primates, genus *Cebus*). *PLoS One* 7:e40398.
- Manly B.F.J. 2007. Randomization, bootstrap and Monte Carlo methods in biology. Boca Raton (FL): Chapman & Hall/CRC.
- Marcus L.F., Hingst-Zaher E., Zaher H. 2000. Application of landmark morphometrics to skulls representing the orders of living mammals. *Hystrix* 11:27–47.
- Mardia K.V., Kent J.T., Bibby J.M. 1979. *Multivariate analysis*. London: Academic Press.
- Márquez E.J., Knowles L.L. 2007. Correlated evolution of multivariate traits: detecting co-divergence across multiple dimensions. *J. Evol. Biol.* 20:2334–2348.
- Martínez-Abadías N., Esparza M., Sjøvold T., González-José R., Santos M., Hernández M., Klingenberg C.P. 2012. Pervasive genetic integration directs the evolution of human skull shape. *Evolution* 66:1010–1023.
- Martínez-Abadías N., Heuzé Y., Wang Y., Jabs E.W., Aldridge K., Richtsmeier J.T. 2011. FGF/FGFR signaling coordinates skull development by modulating magnitude of morphological integration: evidence from Apert syndrome mouse models. *PLoS One* 6:e26425.
- Martins E.P., Hansen T.F. 1997. Phylogenies and the comparative method: a general approach to incorporating phylogenetic information into the analysis of interspecific data. *Am. Nat.* 149: 646–667, erratum 153:448.
- Marugán-Lobón J. 2010. Combining shape data and traditional measurements with 2B-PLS: testing the covariation between avian brain size and cranial shape variation as an example. In: Elewa A.M.T., editor. *Morphometrics for nonmorphometricians*. Berlin: Springer-Verlag. p. 179–190.
- Marugán-Lobón J., Buscalioni Á.D. 2004. Geometric morphometrics in macroevolution: morphological diversity of the skull in modern avian forms in contrast to some theropod dinosaurs. In: Elewa A.M.T., editor. *Morphometrics: applications in biology and paleontology*. Berlin: Springer. p. 157–173.
- Marugán-Lobón J., Buscalioni Á.D. 2006. Avian skull morphological evolution: exploring exo- and endocranial covariation with two-block partial least squares. *Zoology (Jena)* 109:217–230.
- Marugán-Lobón J., Buscalioni Á.D. 2009. New insight on the anatomy and architecture of the avian neurocranium. *Anat. Rec.* 292: 364–370.

- Mayr G. 2011. Metaves, Mirandornithes, Strisores and other novelties—a critical review of the higher-level phylogeny of neornithine birds. *J. Zool. Syst. Evol. Res.* 49:58–76.
- McArdle B.H., Rodrigo A.G. 1994. Estimating the ancestral states of a continuous-valued character using squared-change parsimony: an analytical solution. *Syst. Biol.* 43:573–578.
- McCane B., Kean M.R. 2011. Integration of parts in the facial skeleton and cervical vertebrae. *Am. J. Orthod. Dentofacial Orthop.* 139:e13–e30.
- McCormack J.E., Harvey M.G., Faircloth B.C., Crawford N.G., Glenn T.C., Brumfield R.T. 2013. A phylogeny of birds based on over 1,500 loci collected by target enrichment and high-throughput sequencing. *PLoS One* 8:e54848.
- Meekangvan P., Barhorst A.A., Burton T.D., Chatterjee S., Schovanec L. 2006. Nonlinear dynamical model and response of avian cranial kinesis. *J. Theor. Biol.* 240:32–47.
- Meloro C., Jones A.G. 2012. Tooth and cranial disparity in the fossil relatives of *Sphenodon* (Rhynchocephalia) dispute the persistent 'living fossil' label. *J. Evol. Biol.* 25:2194–2209.
- Meloro C., Raia P., Piras P., Barbera C., O'Higgins P. 2008. The shape of the manibular corpus in large fissioned carnivores: allometry, function and phylogeny. *Zool. J. Linn. Soc.* 154:832–845.
- Mitteroecker P., Bookstein F.L. 2007. The conceptual and statistical relationship between modularity and morphological integration. *Syst. Biol.* 56:818–836.
- Mitteroecker P., Bookstein F.L. 2008. The evolutionary role of modularity and integration in the hominoid cranium. *Evolution* 62:943–958.
- Mitteroecker P., Gunz P., Bernhard M., Schaefer K., Bookstein F.L. 2004. Comparison of cranial ontogenetic trajectories among great apes and humans. *J. Hum. Evol.* 46:679–698.
- Mitteroecker P., Gunz P., Bookstein F.L. 2005. Heterochrony and geometric morphometrics: a comparison of cranial growth in *Pan paniscus* versus *Pan troglodytes*. *Evol. Dev.* 7:244–258.
- Monteiro L.R. 1999. Multivariate regression models and geometric morphometrics: the search for causal factors in the analysis of shape. *Syst. Biol.* 48:192–199.
- Monteiro L.R. 2013. Morphometrics and the comparative method: studying the evolution of shape. *Hystrix* 24. doi:10.4404/hystrix-24.1-6282 (last accessed May 5 2013).
- Monteiro L.R., Abe A.S. 1997. Allometry and morphological integration in the skull of *Tupinambis merianae* (Lacertilia: Teiidae). *Amphib-Reptilia* 18:397–405.
- Monteiro L.R., Bonato V., dos Reis S.F. 2005. Evolutionary integration and morphological diversification in complex morphological structures: mandible shape divergence in spiny rats (Rodentia, Echimyidae). *Evol. Dev.* 7:429–439.
- Monteiro L.R., Nogueira M.R. 2010. Adaptive radiations, ecological specialization, and the evolutionary integration of complex morphological structures. *Evolution* 64:724–744.
- Monteiro L.R., Nogueira M.R. 2011. Evolutionary patterns and processes in the radiation of phyllostomid bats. *BMC Evol. Biol.* 11:137.
- Mosimann J.E. 1970. Size allometry: size and shape variables with characterizations of the lognormal and generalized gamma distributions. *J. Am. Stat. Assoc.* 65:930–945.
- Moyle R.G. 2006. A molecular phylogeny of kingfishers (Alcedinidae) with insights into early biogeographic history. *Auk* 123:487–499.
- Muñoz-Muñoz F., Sans-Fuentes M.A., López-Fuster M.J., Ventura J. 2011. Evolutionary modularity of the mouse mandible: dissecting the effect of chromosomal reorganizations and isolation by distance in a Robertsonian system of *Mus musculus domesticus*. *J. Evol. Biol.* 24:1763–1776.
- Neaux D., Guy F., Gilissen E., Coudyzer W., Ducrocq S. 2013a. Covariation between midline cranial base, lateral basicranium, and face in modern humans and chimpanzees: a 3D geometric morphometric analysis. *Anat. Rec.* 296:568–579.
- Neaux D., Guy F., Gilissen E., Coudyzer W., Vignaud P., Ducrocq S. 2013b. Facial orientation and facial shape in extant great apes: a geometric morphometric analysis of covariation. *PLoS One* 8:e57026.
- Noden D.M., Trainor P.A. 2005. Relationships and interactions between cranial mesoderm and neural crest populations. *J. Anat.* 207:575–601.
- Nogueira M.R., Peracchi A.L., Monteiro L.R. 2009. Morphological correlates of bite force and diet in the skull and mandible of phyllostomid bats. *Funct. Ecol.* 23:715–723.
- O'Hara R.J. 1988. Homage to Clio, or, toward an historical philosophy for evolutionary biology. *Syst. Zool.* 37:142–155.
- O'Higgins P., Cobb S.N., Fitton L.C., Gröning F., Phillips R., Liu J., Fagan M.J. 2011. Combining geometric morphometrics and functional simulation: an emerging toolkit for virtual functional analyses. *J. Anat.* 218:3–15.
- Olson E.C., Miller R.L. 1958. Morphological integration. Chicago (IL): University of Chicago Press.
- Pacheco M.A., Battistuzzi F.U., Lentino M., Aguilar R.F., Kumar S., Escalante A.A. 2011. Evolution of modern birds revealed by mitogenomics: timing the radiation and origin of major orders. *Mol. Biol. Evol.* 28:1927–1942.
- Parsons T.E., Schmidt E.J., Boughner J.C., Jamniczky H.A., Marcucio R.S., Hallgrímsson B. 2011. Epigenetic integration of the developing brain and face. *Dev. Dyn.* 240:2233–2244.
- Pavlicev M., Cheverud J.M., Wagner G.P. 2009. Measuring morphological integration using eigenvalue variance. *Evol. Biol.* 36:157–170.
- Pearson K. 1901. On lines and planes of closest fit to systems of points in space. *Philos. Mag. J. Sci.* 2:559–572.
- Perez S.I., Klaczko J., Rocatti G., dos Reis S.F. 2011. Patterns of cranial shape diversification during the phylogenetic branching process of New World monkeys (Primates: Platyrrhini). *J. Evol. Biol.* 24:1826–1835.
- Phillips M.J., Gibb G.C., Crimp E.A., Penny D. 2010. Tinamous and moa flock together: mitochondrial genome sequence analysis reveals independent losses of flight among ratites. *Syst. Biol.* 59:90–107.
- Pierce S.E., Angielczyk K.D., Rayfield E.J. 2008. Patterns of morphospace occupation and mechanical performance in extant crocodylian skulls: a combined geometric morphometric and finite element modeling approach. *J. Morphol.* 269:840–864.
- Pons J.-M., Hassanin A., Crochet P.-A. 2005. Phylogenetic relationships within the *Laridae* (Charadriiformes: *Aves*) inferred from mitochondrial markers. *Mol. Phylogenet. Evol.* 37:686–699.
- Ponssa M.L., Candiotti M.F.V. 2012. Patterns of skull development in anurans: size and shape relationship during postmetamorphic cranial ontogeny in five species of the *Leptodactylus fuscus* group (Anura: Leptodactylidae). *Zoomorphology (Berl.)* 131:349–362.
- Porto A., De Oliveira F.B., Shirai L.T., De Conto V., Marroig G. 2009. The evolution of modularity in the mammalian skull I: morphological integration patterns and magnitudes. *Evol. Biol.* 36:118–135.
- Purvis A., Garland T. Jr. 1993. Polytomies in comparative analyses of continuous characters. *Syst. Biol.* 42:569–575.
- Rayfield E.J. 2011. Strain in the ostrich mandible during simulated pecking and validation of specimen-specific finite element models. *J. Anat.* 218:47–58.
- Renaud S., Alibert P., Auffray J.-C. 2012. Modularity as a source of new morphological variation in the mandible of hybrid mice. *BMC Evol. Biol.* 12:141.
- Revell L.J. 2009. Size-correction and principal components for interspecific comparative studies. *Evolution* 63:3258–3268.
- Revell L.J., Harmon L.J. 2008. Testing quantitative genetic hypotheses about the evolutionary rate matrix for continuous characters. *Evol. Ecol. Res.* 10:311–331.
- Rodríguez-Mendoza R., Muñoz M., Saborido-Rey F. 2011. Ontogenetic allometry of the bluemouth, *Helicolenus dactylopterus dactylopterus* (Teleostei: Scorpaenidae), in the Northeast Atlantic and Mediterranean based on geometric morphometrics. *Hydrobiologia* 670:5–22.
- Rohlf F.J. 2001. Comparative methods for the analysis of continuous variables: geometric interpretations. *Evolution* 55:2143–2160.
- Rohlf F.J. 2006. A comment on phylogenetic correction. *Evolution* 60:1509–1515.
- Rohlf F.J., Corti M. 2000. The use of two-block partial least-squares to study covariation in shape. *Syst. Biol.* 49:740–753.
- Rosas A., Bastir M. 2004. Geometric morphometric analysis of allometric variation in the mandibular morphology of the hominids of Atapuerca, Sima de los Huesos site. *Anat. Rec.* 278A:551–560.

- Sallan L.C., Friedman M. 2012. Heads or tails: staged diversification in vertebrate evolutionary radiations. *Proc. R. Soc. Lond. B Biol. Sci.* 279:2025–2032.
- Sanger T.J., Mahler D.L., Abzhanov A., Losos J.B. 2012. Roles for modularity and constraint in the evolution of cranial diversity among *Anolis* lizards. *Evolution* 66:1525–1542.
- Schlusser G., Wagner G.P. 2004. Modularity in development and evolution. Chicago (IL): University of Chicago Press. p. x + 600.
- Sheldon F.H., Jones C.E., McCracken K.G. 2000. Relative patterns and rates of evolution in heron nuclear and mitochondrial DNA. *Mol. Biol. Evol.* 17:437–450.
- Shirai L.T., Marroig G. 2010. Skull modularity in Neotropical marsupials and monkeys: size variation and evolutionary constraint and flexibility. *J. Exp. Zool. B Mol. Dev. Evol.* 314:663–683.
- Sidlauskas B. 2008. Continuous and arrested morphological diversification in sister clades of characiform fishes: a phylomorphospace approach. *Evolution* 62:3135–3156.
- Sidlauskas B.L., Mol J.H., Vari R.P. 2011. Dealing with allometry in linear and geometric morphometrics: a taxonomic case study in the *Leporinus cylindriciformis* group (Characiformes: Anostomidae) with description of a new species from Suriname. *Zool. J. Linn. Soc.* 162:103–130.
- Sievwright H., Higuchi H. 2011. Morphometric analysis of the unusual feeding morphology of Oriental Honey Buzzards. *Ornithol. Sci.* 10:131–144.
- Singh N., Harvati K., Hublin J.-J., Klingenberg C.P. 2012. Morphological evolution through integration: a quantitative study of cranial integration in *Homo*, *Pan*, *Gorilla* and *Pongo*. *J. Hum. Evol.* 62: 155–164.
- Strand Viðarsdóttir U., O'Higgins P., Stringer C.B. 2002. A geometric morphometric study of regional differences in the ontogeny of the modern human facial skeleton. *J. Anat.* 201:211–229.
- Sydney N.V., Machado F.A., Hingst-Zaher E. 2012. Timing of ontogenetic changes of two cranial regions in *Sotalia guianensis* (Delphinidae). *Mamm. Biol.* 77:397–403.
- Tabachnick R.E., Bookstein F.L. 1990. The structure of individual variation in Miocene *Globorotalia*. *Evolution* 44:416–434.
- Tokita M., Takuya K., Armstrong K.N. 2007. Evolution of craniofacial novelty in parrots through developmental modularity and heterochrony. *Evol. Dev.* 9:590–601.
- Treplin S., Siegert R., Bleidorn C., Thompson H.S., Fotsó R., Tiedemann R. 2008. Molecular phylogeny of songbirds (Aves: Passeriformes) and the relative utility of common nuclear marker loci. *Cladistics* 24:328–349.
- Tucker L.R. 1958. An inter-battery method of factor analysis. *Psychometrika* 23:111–136.
- van der Meij M.A.A., Bout R.G. 2008. The relationship between shape of the skull and bite force in finches. *J. Exp. Biol.* 211:1668–1680.
- Wagner G.P. 1984. On the eigenvalue distribution of genetic and phenotypic dispersion matrices: evidence for a nonrandom organization of quantitative character variation. *J. Math. Biol.* 21:77–95.
- Wagner G.P. 1996. Homologues, natural kinds and the evolution of modularity. *Am. Zool.* 36:36–43.
- Wagner G.P., Altenberg L. 1996. Complex adaptations and the evolution of evolvability. *Evolution* 50:967–976.
- Webster M., Zelditch M.L. 2011. Modularity of a Cambrian ptychoparioid trilobite cranidium. *Evol. Dev.* 13:96–109.
- Weisensee K.E., Jantz R.L. 2011. Secular change in craniofacial morphology of the Portuguese using geometric morphometrics. *Am. J. Phys. Anthropol.* 145:548–559.
- Wellens H.L.L., Kuijpers-Jagtman A.M., Halazonetis D.J. 2013. Geometric morphometric analysis of craniofacial variation, ontogeny and modularity in a cross-sectional sample of modern humans. *J. Anat.* 222:397–409.
- Willmore K.E., Leamy L., Hallgrímsson B. 2006. Effects of developmental and functional interactions on mouse cranial variability through late ontogeny. *Evol. Dev.* 8:550–567.
- Wink M., Heidrich P. 2000. Molecular systematics of owls (*Strigiformes*) based on DNA-sequences of the mitochondrial cytochrome b gene. In: Chancellor R.D., Meyburg B.-U., editors. *Raptors at risk*, WWWGBP/Hancock House. p. 819–828.
- Wright T.F., Schirtzinger E.E., Matsumoto T., Eberhard J.R., Graves G.R., Sanchez J.J., Capelli S., Müller H., Scharpegge J., Chambers G.K., Fleischer R.C. 2008. A multilocus molecular phylogeny of the parrots (Psittaciformes): support for a Gondwanan origin during the Cretaceous. *Mol. Biol. Evol.* 25:2141–2156.
- Wroe S., Milne N. 2007. Convergence and remarkably consistent constraint in the evolution of carnivore skull shape. *Evolution* 61:1251–1260.
- Young N.M. 2006. Function, ontogeny and canalization of shape variance in the primate scapula. *J. Anat.* 209:623–636.
- Young R.L., Badyaev A.V. 2006. Evolutionary persistence of phenotypic integration: influence of developmental and functional relationships on complex trait evolution. *Evolution* 60:1291–1299.
- Zelditch M.L., Wood A.R., Bonett R.M., Swiderski D.L. 2008. Modularity of the rodent mandible: integrating bones, muscles, and teeth. *Evol. Dev.* 10:756–768.
- Zusi R.L. 1993. Patterns of diversity in the avian skull. In: Hanken J., Hall B.K., editors. *The skull*. Vol. 2: Patterns of structural and systematic diversity. Chicago (IL): University of Chicago Press. p. 391–437.